European Journal of Medicinal Chemistry 265 (2024) 116053

Contents lists available at ScienceDirect

European Journal of Medicinal Chemistry

journal homepage: www.elsevier.com/locate/ejmech

Research paper

Pyrrolopyrimidine based CSF1R inhibitors: Attempted departure from Flatland

Frithjof Bjørnstad [a,b], Simen Havik [a], Thomas Ihle Aarhus [a,c], Iktedar Mahdi [a], Anke Unger [c], Peter Habenberger [c], Carsten Degenhart [c], Jan Eickhoff [c], Bert M. Klebl [c], Eirik Sundby [b], Bård Helge Hoff [a,*]

[a] Department of Chemistry, Norwegian University of Science and Technology (NTNU), Høgskoleringen 5, NO-7491, Trondheim, Norway
[b] Department of Material Science, Norwegian University of Science and Technology (NTNU), NO-7491, Trondheim, Norway
[c] Lead Discovery Center GmbH (LDC), Otto-Hahn-Strasse 15, 44227, Dortmund, Germany

ARTICLE INFO

Keywords:
CSF1R inhibitors
Tetrahydropyran
Pyrrolopyrimidine
Kinase profiling
PLX3397

ABSTRACT

The colony-stimulating factor 1 receptor (CSF1R) is an attractive target for inflammation disorders and cancers. Based on a series of pyrrolo[2,3-*d*]pyrimidine containing two carbo-aromatic rings, we have searched for new CSF1R inhibitors having a higher fraction of sp^3-atoms. The phenyl unit in the 4-amino group could efficiently be replaced by tetrahydropyran (THP) retaining inhibitor potency. Exchanging the 6-aryl group with cyclohex-2-ene units also resulted in highly potent compounds, while fully saturated ring systems at C-6 led to a loss of activity. The structure-activity relationship study evaluating THP containing pyrrolo[2,3-*d*]pyrimidine derivates identified several highly active inhibitors by enzymatic studies. A comparison of 11 pairs of THP and aromatic compounds showed that inhibitors containing THP had clear benefits in terms of enzymatic potency, solubility, and cell toxicity. Guided by cellular experiments in Ba/F3 cells, five CSF1R inhibitors were further profiled in ADME assays, indicating the *para*-aniline derivative **16t** as the most attractive compound for further development.

1. Introduction

The colony-stimulating factor 1 receptor (CSF1R) is a tyrosine kinase expressed on the monocyte/macrophage lineages and bone resorbing osteoclasts [1,2]. Binding of the cytokines colony-stimulating factor 1 (CSF-1) and interleukin 34 (IL-34) leads to activation of CSF1R and downstream signalling, which is necessary for normal function and differentiation of macrophages, microglia and osteoclasts. However, in some diseases, overexpression of CSF-1 and/or elevated activity of CSF1R cause a misbalance of the immune cell phenotypes [3]. A working hypothesis is that efficient and selective CSF1R inhibitors in some indications can re-educate the cells to a more balanced level of phenotypes. Thus, CSF1R inhibitors might be relevant in cancers [4], CNS-diseases [5,6], and bone diseases [7]. As of 2023, there is one FDA approved small molecule CSF1R inhibitor available: Pexidartinib (PLX3397), sold under the brand name Turalio™ as a treatment for tenosynovial giant cell tumours. Additionally, HMPL-012 has been approved for use in China [8]. Other low molecular weight inhibitors are also undergoing clinical trials [8,9]. Some examples are Vimseltinib (DCC-3014) [10], Sotuletinib (BLZ945) [11], PRV-6527 [12], and ABT-869 [13]. An interesting inhibitor is also IACS-9429 derived from Sotuletinib [14]. These structures are shown in Fig. 1.

Recently our group identified CSF1R inhibitors based on the pyrrolopyrimidine scaffold [15,16], see Fig. 1. These compounds contain two carbon aromatic substituents, important for activity. However, drug candidates based on carbon aromatics can have several drawbacks and it has been found that if the fraction of sp^3 carbons is increased, the likelihood of clinical success is increased [17–19]. This has triggered synthetic efforts towards aliphatic building blocks for replacing aromatic structures [20–23]. Possible benefits of transitioning form aromatic to sp^3 based structures include increased solubility by disrupting molecular planarity/crystallinity [24], and higher specificity due to more intimate and unique ligand-protein contacts. Additionally, increasing the number of sp^3 carbons may enhance metabolic stability and reduce cell toxicity. A drawback could be more rotational bonds causing larger entropy loss on ligand binding. Interestingly, the CSF1R inhibitors BLZ945 and

* Corresponding author. Department of Chemistry, Norwegian University of Science and Technology, Høgskoleringen 5,7491, Trondheim, Norway.
E-mail address: bard.h.hoff@ntnu.no (B.H. Hoff).

https://doi.org/10.1016/j.ejmech.2023.116053
Received 9 November 2023; Received in revised form 8 December 2023; Accepted 11 December 2023
Available online 17 December 2023

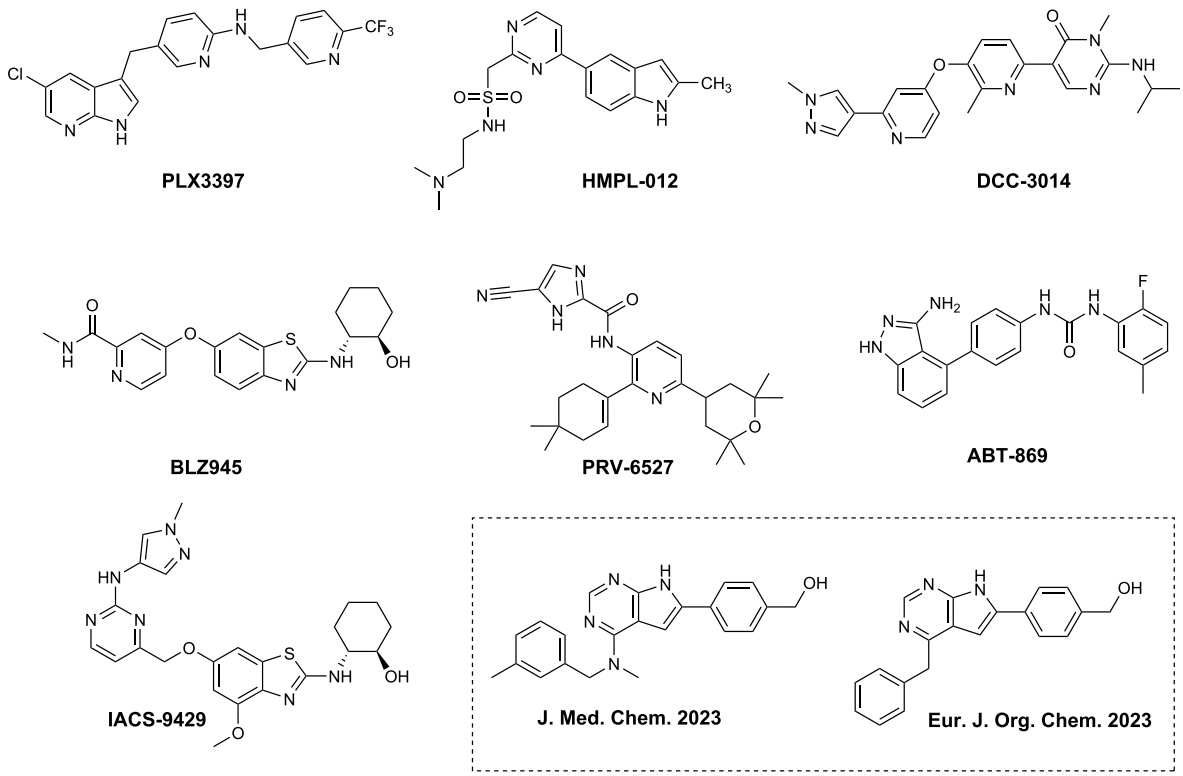

Fig. 1. CSF1R inhibitors undergoing clinical trials, the discovery compound IACS-9429 and pyrrolopyrimidine based inhibitors [15,16].

PRV-6527 have a relative high number of saturated carbons in their structure. Herein, we describe our efforts to replace two aromatic ring systems with sp^3 based substituents for a class of CSF1R inhibitors.

2. Result and discussion

2.1. Design of the study

In our previous studies on CSF1R inhibitors we have identified both 4,6-disubstituted pyrrolopyrimidines [15,16], and 6,8-disubstituted purines [25] to be potent CSF1R inhibitors in enzymatic studies. Hurdles for progression of these molecules to *in vivo* efficacy studies were metabolic stability, and low solubility. In the purine series of compounds, we discovered that the tetrahydropyran (THP) unit efficiently improved solubility and CSF1R inhibitory potency. Thus, we aimed at investigating the effect of various non-aromatic amines at C-4 also in the pyrrolopyrimidine series. Additionally, we wanted to explore the effect of exchanging the aromatic structures at C-6 with other 6-membered rings, see Scheme 1.

2.2. Chemistry

Initially, we synthesized the simple pyrrolopyrimidines **16a-22a** following the route outlined in Scheme 2. Regioselective amination of **1** gave the 4-substituted analogues **2–8** in 47–98 % yield. Then a Suzuki–Miyaura cross-coupling with $PdCl_2$-dppf in dioxane/water provided the 4,6-disubstituted derivatives **9a-15a** (67–91 % isolated yield). Deprotection of the SEM group gave mediocre yields for **18** (58 %) and **21** (44 %). During the reaction, formaldehyde is released. Thus, hydroxymethylation can then occur on electron rich aromatic positions, and the hydroxymethyl derivative **23** was isolated as a side product. We suspect that similar side products caused difficulties in purification for some of the compounds. The other derivatives were obtained in 79–95 % yield.

As compound **16a** was most promising in CSF1R inhibition studies and had a favourable solubility, a series of compounds based on intermediate **2** was prepared, see Scheme 3. The Suzuki–Miyaura cross-couplings proceeded mostly in excellent yields. Also, the SEM deprotection allowed for facile isolation of end products in most cases,

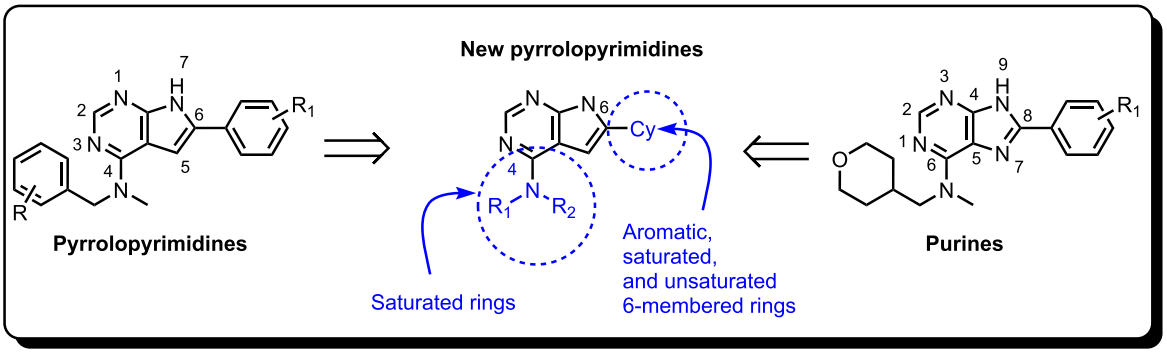

Scheme 1. Investigation of effect of various saturated structures at C-4 and ring systems at C-6 for CSF1R inhibition. The numbering system of the heterocycles are also shown.

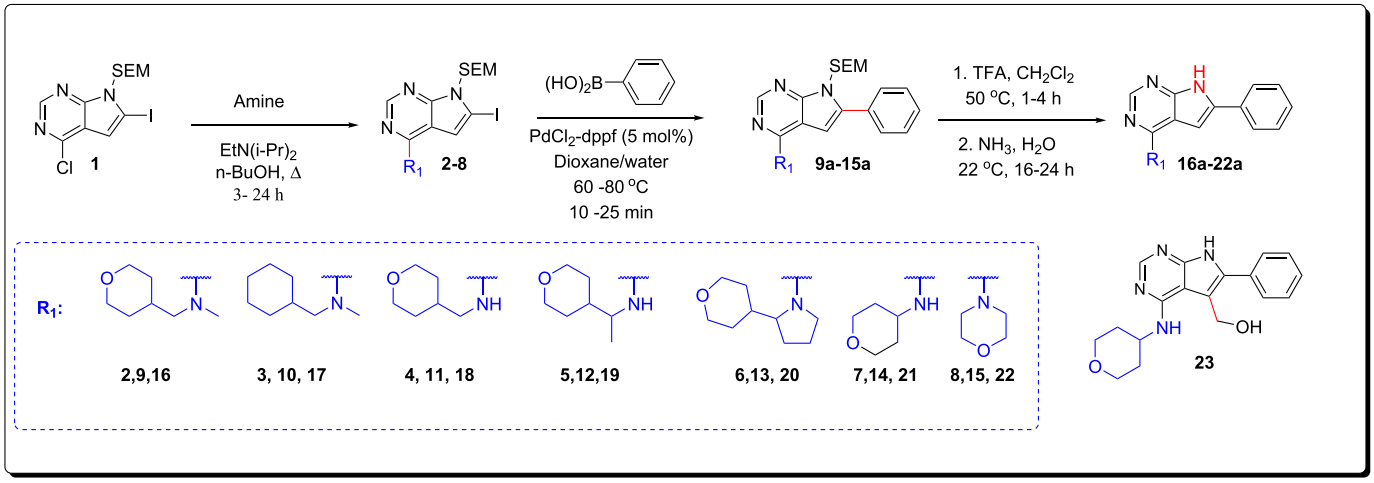

Scheme 2. Synthesis of **16a-22a** starting from building block **1.** The structure of the side product **23** is also shown.

although some challenges were encountered with more electron rich compounds as the methoxy and phenolic derivatives **16c** and **16d**. Post modifications provided additional materials. The carboxylic acid **16s** was obtained from the corresponding methyl ester **16i**, while the aniline derivatives **16t-u** were prepared by iron catalysed reduction. The two amides **16v** and **16w** were made by reactions with the appropriate acid

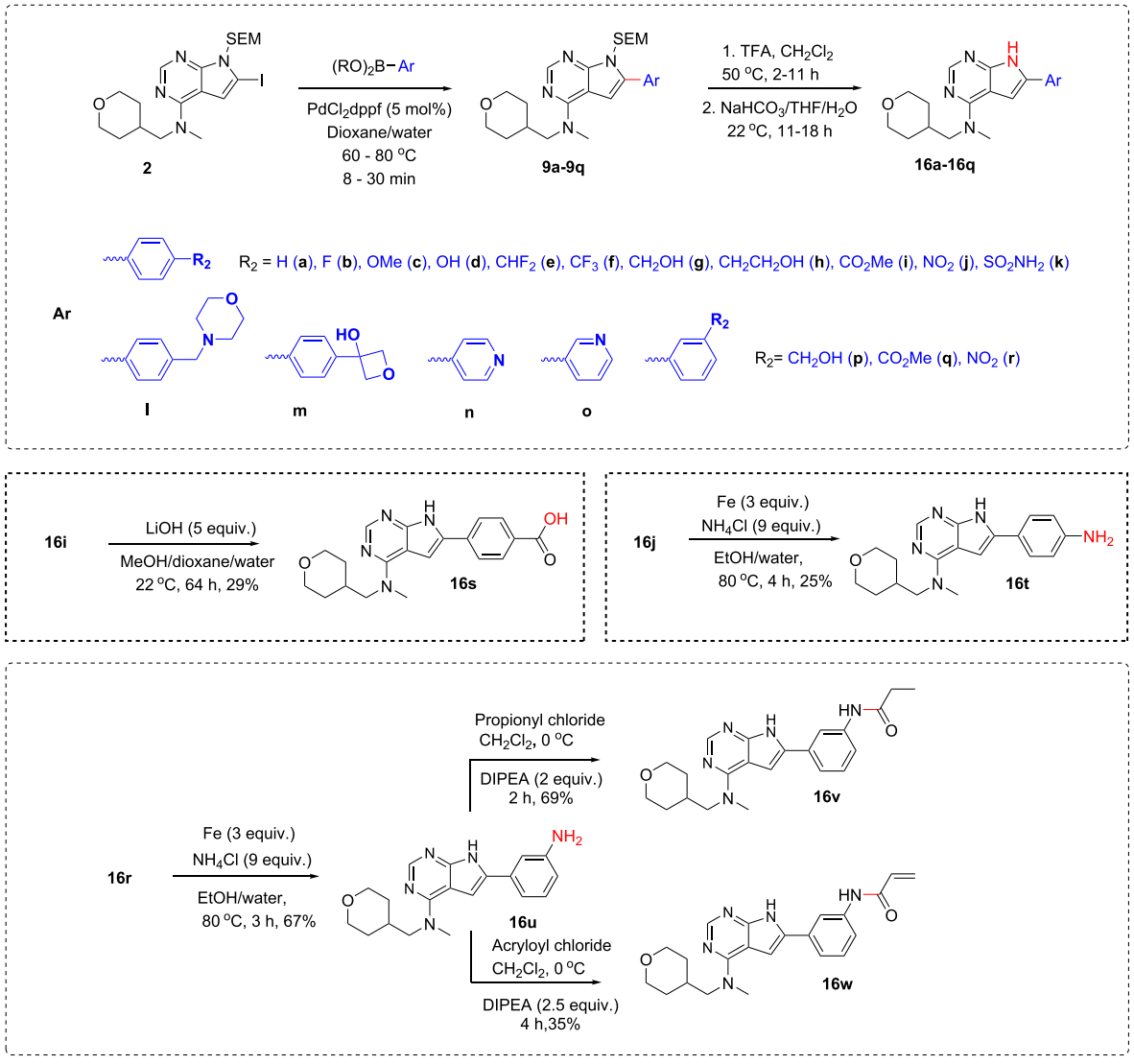

Scheme 3. Synthesis of the CSF1R inhibitor candidates **16a-w**.

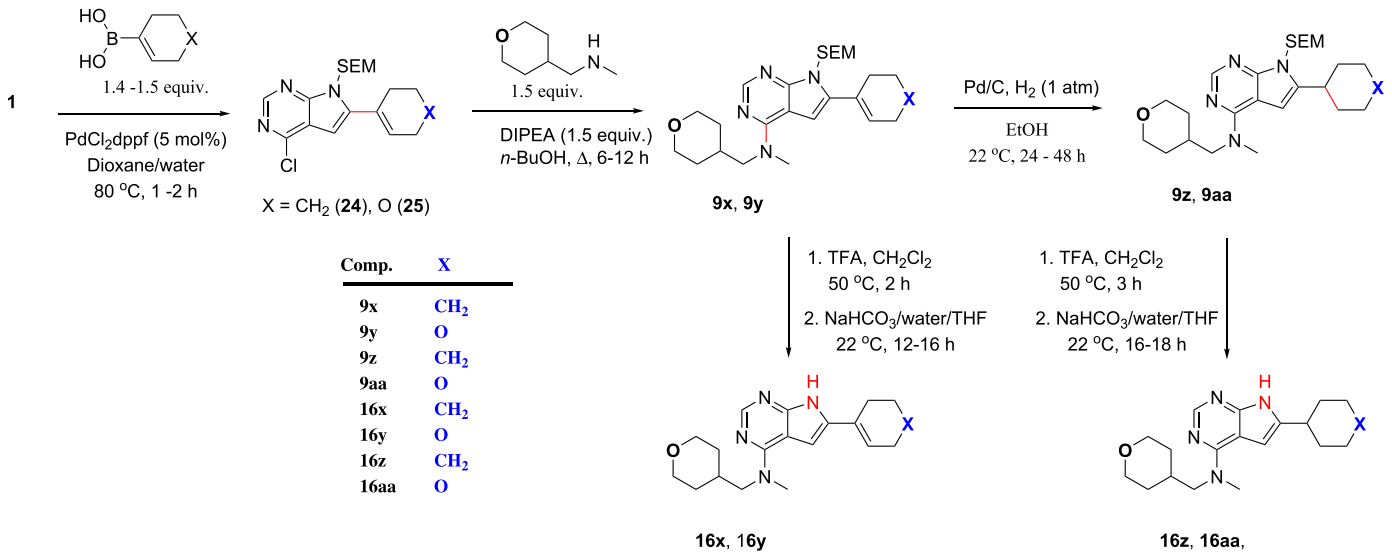

Comp.	X
9x	CH_2
9y	O
9z	CH_2
9aa	O
16x	CH_2
16y	O
16z	CH_2
16aa	O

Scheme 4. Synthesis of **16x, 16y, 16z** and **16aa** initiated by a chemoselective Suzuki-Miyaura cross-coupling.

chlorides. Apparently, amides at N-7 are very unstable and tend to convert easily to the wanted compound. For the corresponding 5-arylated pyrrolopyrimidines, we introduced a mild hydrolytic step to cleave the N-7 amides [26], but this was not done in this series.

Some alternative ring systems at C-6 was also installed, starting with a chemoselective Suzuki–Miyaura cross-coupling with cyclohex-1-en-1-ylboronic acid and (3,6-dihydro-2*H*-pyran-4-yl)boronic acid, see Scheme 4. This yielded the cyclohexene and the dihydro-2*H*-pyran derivatives **24** and **25**. Further, amination at C-4 with the THP amine gave **9x-y**. These compounds were reduced to the saturated analogue **9z** and **9aa**.

Deprotection of both the saturated and unsaturated analogues gave **16x - 16aa**. To avoid the use of these expensive alkenyl boronic acids, directed lithiation of **1** and quenching with ketones can be done [27]. The supporting information file shows some examples of this chemistry. It should also be mentioned that attempted hydrogenation of **24** using H_2/Pd, also reduced off the chlorine at C-4.

2.3. CSF1R inhibitory properties

2.3.1. Effect of different amines on CSF1R enzymatic activity

Firstly, seven pyrrolopyrimidines having a phenyl at C-6, and different THP amines and 1-cyclohexyl-*N*-methylmethanamine at C-4, were evaluated for their inhibitory properties. Table 1 shows the CSF1R enzymatic inhibition data using two different assay formats, the calculated logP, the topological polar surface area and the measured solubility. Included is also data for the aromatic analogue having the same number of heavy atoms (compound **26**) and the more potent *meta*-methyl derivative **27a** [16], which is most relevant for comparing potency. Evaluating this series showed that the THP containing compound **16a** and racemic **20a** had high activity in both enzymatic assays, while the cyclohexyl derivative **17a** was less potent at higher ATP

Table 1
CSF1R enzymatic IC_{50}-values using two different assay formats, solubility, the estimated logP (cLogP) and topological polar surface area (TPSA).

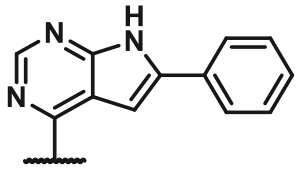

Comp.	Structure	cLogP[a)]	TPSA[b)]	Sol.[c)]	IC_{50} (nM)[d)] (ATP: 10 μM)	IC_{50} (nM)[e)] (ATP: 25 μM)
16a	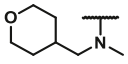	3.0	54	44	0.6 ± 0.0	<3
17a	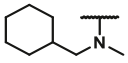	4.2	45	<1	1.5 ± 0.2	15 (0.975)
18a	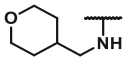	2.8	63	194	17 ± 2	89 (0.993)
19a	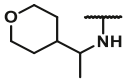	3.1	63	363	111 ± 18	204 (0.990)

(*continued on next page*)

Table 1 (*continued*)

Comp.	Structure	cLogP[a)]	TPSA[b)]	Sol.[c)]	IC_{50} (nM)[d)] (ATP: 10 μM)	IC_{50} (nM)[e)] (ATP: 25 μM)
20a	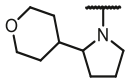	3.5	54	109	2.6 ± 0.7	6 (0.957)
21a	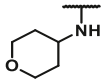	2.6	63	17	60 ± 16	99 (0.997)
22a		2.2	54	9.6	22 ± 4	171 (0.972)
26a[f)]	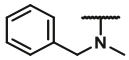	3.8	45	3.1	15 ± 1	20 (0.996)
27a[f)]	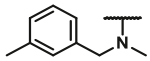	4.2	45	1.9	1.8 ± 0.1	4 (0.947)

[a] Calculated logP estimated using DataWarrior, Version 5.5.0.
[b] Topological polar surface area (TPSA) was estimated using DataWarrior, Version 5.5.0. (Erlich approach).
[c] Kinetic solubility (μM) determined spectrophotometrically at pH 7.4 in HEPES buffer.
[d] Enzymatic IC_{50} values obtained by 10-point titrations in duplicates (20 data points) using Z-LYTE assay platform (ThermoFisher) with standard deviation [28]. ATP concentration is equal to K_M ca. 10 μM.
[e] Enzymatic IC_{50} values obtained by single 8-point titrations using TR-FRET-based LANCE Ultra assay (PerkinElmer), ATP concentration: 25 μM. Goodness of fit (R^2) for the regression is shown in parentheses.
[f] Data from Aarhus et al. [16].

concentration. Relatively low enzymatic inhibitory activity was noted for the other derivatives. The large variance in activity for this series, shows that the detailed structure of the amine is highly important. Moreover, the two assay formats yield similar ranking of compound potency. The initial set of data convinced us that a switch from phenyl based (comp. **26a** and **27a**) to THP (comp. **16a**) allows for more active inhibitors also possessing a higher polarity. This might aid further development. The fraction of sp^3 carbons in moving from the reference structures **26a** and **27a** to **16a** goes from 0.10 and 0.14 to 0.37. Although, the activity of the racemic derivatives **20a**, could have been improved by preparing enantiopure analogues, we selected **16a** as the base for continuing the structure–activity relationship studies.

2.3.2. *Effect of varying the C-6 position*

Further activity optimization was based on the THP scaffold present in **16a**. Some additional compounds containing other amines at C-4 prepared as controls, are shown the Supporting Information File (Table S1). The 30 new inhibitor candidates were profiled in three CSF1R enzymatic assays with different ATP concentration. This was done to evaluate how the ATP level affected inhibitor performance. Most of the compounds were also assayed in a CSF1R Ba/F3 cellular assay and in an IL-3 dependent Ba/F3 (CSF1R independent) assay to indicate cellular toxicity. The results are summarised in Table 2 (*para*-substituted) and Table 3 (other variants).

A relatively large variance in structure at C-6 is allowed for without losing too much enzymatic activity (Tables 2 and 3). The parent compound **16a** and the *para*-fluoro derivative **16b** maintained a high potency at high ATP concentration. However, **16a** was judged to be toxic, while the *para*-fluoro derivative **16b**, unfortunately had low activity towards the CSF1R Ba/F3 cells.

The *para*-methoxy **16c** and *para*-hydroxyl **16d** appeared promising in both enzymatic and cell assays. Incorporation of fluorines can be beneficial for blocking metabolism [29,30], thus the difluoromethyl and trifluoromethyl derivatives **16e** and **16f** were prepared. While the enzymatic activity was promising, the difluoromethyl analogue **16e** was only moderately active in cells (IC_{50} = 5.5 μM), while the trifluoromethyl **16f** was inactive.

We have previously found the *para*-hydroxymethyl and *para*-hydroxyethyl groups to be potency inducing substituents in enzymatic assays [25], and this was also the case here for derivatives **16g** and **16h**. The highest cell activity was seen for the *para*-hydroxyethyl analogue **16h**. The methyl ester **16i**, the nitro derivative **16j** and the sulphonamide **16k** performed poorly in the Ba/F3 cell system. A morpholine substituent was also inserted (compound **16l**). For this compound the CSF1R Ba/F3 activity seemed promising, but a surprisingly low solubility did not allow for accurate evaluation in the Ba/F3 control cells. We have previously observed compounds containing *para*-hydroxymethyl to be metabolically labile [25]. Interestingly, bioisosteric replacement to the oxetane containing **16m**, showed to be the most potent compound in the Ba/F3 cellular assay. The binding mode of this inhibitor as indicated by docking is shown in Fig. 2. Interestingly, the endocyclic oxygen of the oxetane appears to interact with Lys586 as a hydrogen bond acceptor.

Based on the enzymatic profiling we also had high hopes for the benzoic acid **16s**. Disappointingly, the compound was inactive in the Ba/F3 cell assay. Acidic compounds tend to have lower permeability than neutral and anionic molecules [31], and a follow up MDCK permeability assay indicated a low rate of transfer in the A to B direction (1.9×10^{-6} cm/s) to be a possible cause (data not shown). The *para*-aniline **16t** on the other hand showed promising Ba/F3 cell activity (IC_{50} = 1.2 μM). The docked structure had similar binding mode as **16m**, Fig. 3. Additionally, a cation-π interaction was identified between the electron rich C-6 aryl and Lys586.

The data for other substitution patterns at C-6 is shown in Table 3. A way to avoid oxidative metabolism at aromatics is to reduce the electron density by switching to pyridyls, and as seen in Fig. 1, pyridine units are a common element in CSF1R inhibitors. Unfortunately, both the 4-pyridyl **16n** and the 3-pyridyl **16o** had mediocre cell activity. Six *meta*-substituted analogues were profiled. The hydroxymethyl **16p**, the methyl ester **16q**, and the nitro derivative **16r** all had mediocre Ba/F3 cellular activity, but higher than for the corresponding *para*-derivatives. The effect is difficult to rationalize as the molecular properties and enzyme inhibition data are rather similar. The *meta*-aniline **16u** appeared to have some cellular off-targets as evidenced by the Ba/F3 control cell line. Amides are common drug motifs. The propionamide **16v** showed promising enzymatic IC_{50}, while the Ba/F3 IC_{50} was only 5.5 μM. The corresponding acrylate structure **16w**, with a Michael

Table 2
Enzymatic IC_{50} values and profiling in BA/F3 cells for *para*-substituted compounds (**16a-t**).

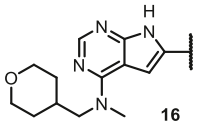

16

Comp.	Group	Enzymatic assay			Cellular assay	
		IC_{50} (nM)[a] (ATP: 10 μM)	IC_{50} (nM)[b] (ATP: 25 μM)	IC_{50} (nM)[c] (ATP: 2.5 mM)	IC_{50} (μM), Ba/F3 CSF1R[d]	IC_{50} (μM), Ba/F3 IL-3[e]
16a		0.6 ± 0.0	<3	6 (0.979)	1.1 ± 0.2	1.7
16b	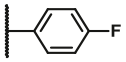	0.8 ± 0.1	<3	7 (0.982)	7.1 ± 1.9	>9.9
16c	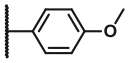	0.4 ± 0.1	<3	<3	1.4±0.5	>9.9
16d	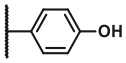	0.3 ± 0.1	8 (0.989)	11 (0.995)	1.2 ± 0.5	>9.9
16e	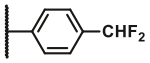	0.8 ± 0.1	<3	ND[f]	4.7 ± 1.8	>9.9
16f	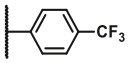	1.9 ± 0.2	6 (0.906)	29 (0.949)	>9.9	>9.9
16g	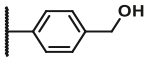	0.5 ± 0.1	<3	5 (0.978)	3.1 ± 0.6	>9.9
16h	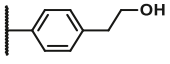	<0.3	<3	<0.3	1.5 ± 0.3	>9.9
16i	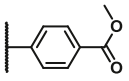	1.5 ± 0.2	3 (0.890)	18 (0.993)	>9.9	>9.9
16j	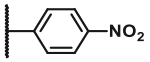	0.7 ± 0.1	12 (0.991)	29 (0.954)	>9.9	>9.9
16k	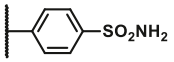	<0.3	<3	ND[f]	6.9 ± 2.5	>9.9
16l	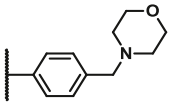	<0.3	<3	6 (0.987)	>1[g]	>1[g]
16m	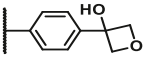	<0.3	<3	ND[f]	0.51 ± 0.0	>9.9
16s	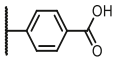	0.4 ± 0.0	<3	6 (0.990)	>9.9	>9.9
16t	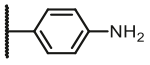	0.3 ± 0.2	3	6 (0.990)	1.2 ± 0.3	>9.9
PLX-3397		4.7 ± 2.0	13 ± 4	35 (0.998)	0.06 ± 0.01	>9.9

[a] Enzymatic IC_{50} values obtained by 10-point titrations) using Z-LYTE assay platform (ThermoFisher) [28] with standard deviation. ATP concentration is equal to K_M ca. 10 μM.
[b] Enzymatic IC_{50} values obtained by single 8-point titrations using TR-FRET-based LANCE Ultra assay (PerkinElmer), ATP concentration: 25 μM. Goodness of fit (R^2) for the regression is shown in parentheses.
[c] Enzymatic IC_{50} values obtained by by single 8-point titrations using TR-FRET-based LANCE Ultra assay (PerkinElmer), ATP concentration: 2.5 mM. Goodness of fit (R^2) for the regression is shown in parentheses.
[d] Cellular assay of Ba/F3 cells engineered to be dependent on CSF1R.
[e] Cellular assay of Ba/F3 cells engineered to be dependent on IL-3.
[f] Not determined (ND).
[g] Low solubility made analysis difficult.

Table 3
Enzymatic IC_{50} values and profiling in Ba/F3 cells for other substituents at C-6 (**16n** - **16aa**).

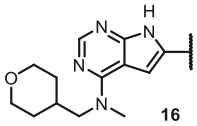

16

Comp.	Group	Enzymatic assay			Cellular assay	
		IC_{50} (nM)[a] (ATP: 10 μM)	IC_{50} (nM)[b] (ATP: 25 μM)	IC_{50} (nM)[c] (ATP: 2.5 mM)	IC_{50} (μM), Ba/F3 CSF1R[d]	IC_{50} (μM), Ba/F3 IL-3[e]
16n		1.1 ± 0.2	13 (0.998)	48 (0.997)	4.0 ± 1.2	>9.9
16o		1.4 ± 0.2	3 (0.971)	18 (0.995)	3.1 ± 0.2	8.8
16p	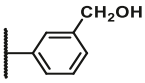	0.6 ± 0.1	6 (0.984)	12 (0.998)	1.9 ± 0.5	>9.9
16q	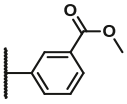	2.2 ± 0.2	3 (0.995)	24 (0.993)	4.5 ± 0.5	9.2
16r	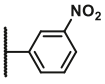	2.7 ± 0.4	14 (0.961)	43 (0.984)	7.3 ± 1.3	>9.9
16u	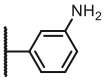	0.4 ± 0.1	<3	4 (0.987)	2.0 ± 0.0	5.3
16v	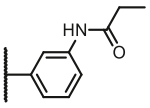	1.2 ± 0.2	<3	13 (0.989)	5.5 ± 0.7	>9.9
16w	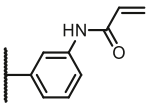	0.5 ± 0.1	17 (0.980)	24 (0.990)	1 ± 0.4	0.5
16x		0.4 ± 0.0	6 (0.986)	12 (0.999)	1.2 ± 0.3	>9.9
16y		0.4 ± 0.2	<3	ND[f]	2.9 ± 0.6	>9.9
16z		7.9 ± 2.3	152 (0.973)	432 (0.977)	8.9 ± 0.2	>9.9
16aa		15 ± 3	145 (0.955)	562 (0.978)	>9.9	>9.9

[a] Enzymatic IC_{50} values obtained by 10-point titrations in duplicates (20 data points) using Z-LYTE assay platform (ThermoFisher) [28], with standard deviation. ATP concentration is equal to K_M ca. 10 μM.
[b] Enzymatic IC_{50} values obtained by single 8-point titrations using TR-FRET-based LANCE Ultra assay (PerkinElmer), ATP concentration: 25 μM. Goodness of fit (R^2) for the regression is shown in parentheses.
[c] Enzymatic IC_{50} values obtained by single 8-point titrations using TR-FRET-based LANCE Ultra assay (PerkinElmer), ATP concentration: 2.5 mM. Goodness of fit (R^2) for the regression is shown in parentheses.
[d] Cellular assay of Ba/F3 cells engineered to be dependent on CSF1R.
[e] Cellular assay of Ba/F3 cells engineered to be dependent on IL-3.
[f] Not determined (ND).

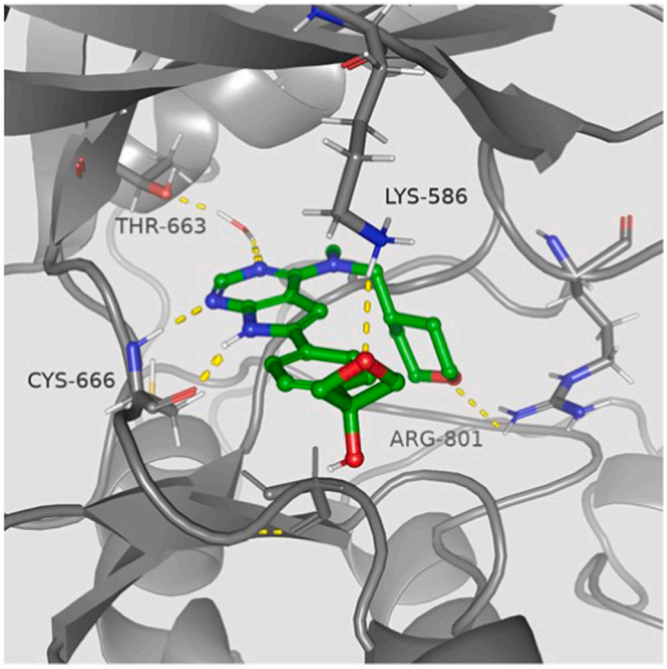

Fig. 2. Binding mode comparison of **16m** (green) docked and superimposed on CSF1R (PDB: 8CGC [16]). Hydrogen bonding between N-1 and N-7 to Cys666, the oxygen in the oxetane ring in **16m** and Lys586 and a water bridge from N3 to Thr663 are shown as yellow dashed lines.

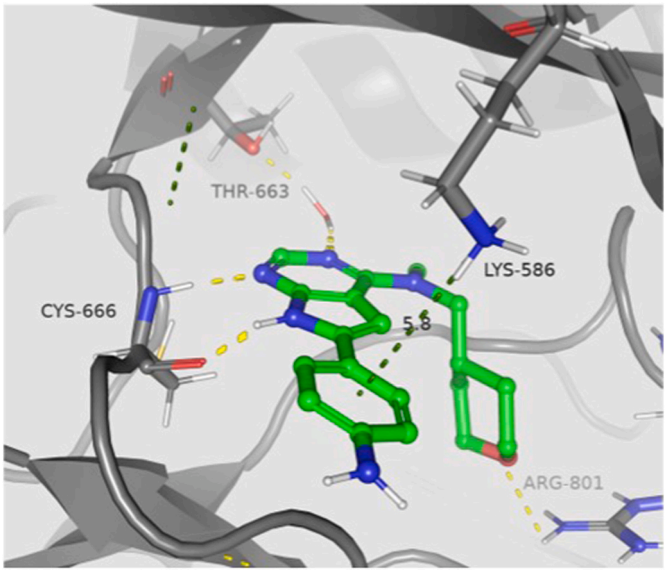

Fig. 3. Binding mode of **16t** (green) docked and superimposed on CSF1R (PDB: 8CGC [16]). Hydrogen bonding between N-1 and N-7 to Cys666, and a water bridge from N3 to Thr663 are shown as yellow dashed lines. The dotted green line indicates a cation-π interaction between Lys586 and the aniline unit in **16t.**

acceptor warhead, was designed to act as an irreversible inhibitor targeting Cys667. Its enzymatic IC_{50} values at elevated ATP concentration was relatively high compared to the best compounds in this series. Thus, we assume that **16w** does not form a covalent bond with Cys667. Not surprisingly, the acrylate **16w** was highly toxic towards the Ba/F3 control cell line. In drug development, it is often beneficial if carbon aromatics are exchanged with saturated structures. This prompted us to prepare derivatives **16x-16aa**. The cyclohexene derivative **16x** and the 3,6-dihydro-2*H*-pyran **16z** (Table 3) had high enzymatic inhibitory

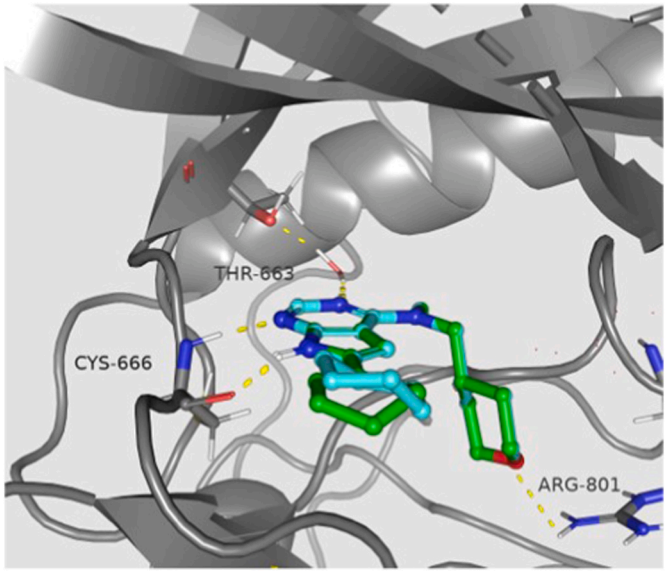

Fig. 4. Compound **16x** (green) and **16z** (sky blue) docked and superimposed on CSF1R (PDB: 8CGC [16]). Hydrogen bonding between N-1 and N-7 to Cys666 and a water bridge from N3 to Thr663 are shown as yellow dashed lines.

activity. Inhibitor **16x** also had a promising IC_{50} of 1.2 μM in the Ba/F3 assay, but as will be evident in the following section, its metabolic stability was inferior.

Upon reduction of the double bond in inhibitors **16x** and **16y**, the saturated analogues lost most of their enzymatic CSF1R activity and cellular activity. The potency reducing effect of the cyclohexyl moiety was also confirmed by preparing an aromatic analogue (see Supporting information, Table S1). A less efficient binding of **16z** compared **16x** was supported by calculations of the corresponding MMGBSA ΔG binding energies using Prime, although *in silico* docking experiments with the target protein (PDB: 8CGC) using the cycloalkene **16x** and saturated analogue **16z** indicated that the central pyrrolopyrimidine unit and the THP-amine exhibited complete superimposition. To further investigate the negative effect of introducing a saturated ring, ab initio conformational searches (Jaguar) around the C6 bond for **16x** and **16y** were done. This showed that the cyclohexene unit in **16x** was preferably oriented out of plane of the pyrrolopyridimine by 20°, while the cyclohexyl unit in **16z** was tilted by 60°. (Supporting information Table S3). However, the torsion of the cyclohexyl at C6 appears slightly unfavourable in the docked structure (Fig. 4) compared to that seen in the conformational search. Cyclohexane groups are also likely to have a higher entropy loss on binding relative to a less flexible cyclohexene unit, which might cause lower binding.

To conclude, the enzymatic studies showed the compounds inhibitory properties to be differently affected by ATP concentration. Most of the antagonists maintained high inhibition even at 2.5 mM ATP. However, a significantly higher IC_{50} was noted at the highest ATP concentration (2.5 mM) for the trifluoromethyl **16f**, the pyridyl **16n**, but also PLX3397. An obvious difference between enzymatic and cellular studies is the ATP concentration which is much higher in cells. Thus, higher cellular ATP concentration might explain the Ba/F3 cellular results for **16f** and **16n**, but likely not for the rest of the compounds. Poor cell membrane permeability is another reason why activity in cells can drop. This is a likely explanation for the low cellular activity of the rather non-polar *para*-fluoro **16b** and *para*-trifluoromethyl **16f** derivatives. Poor ability to penetrate cell walls was also evidenced by MDCK assay in the case of the benzoic acid **16s**. However, for a high number of compounds there is no clear indication what is causing the mediocre cell activity, relative to that seen for PLX3397. The enzymatic CSF1R assays utilized are obviously not an excellent model for CSF1R inhibition in cells.

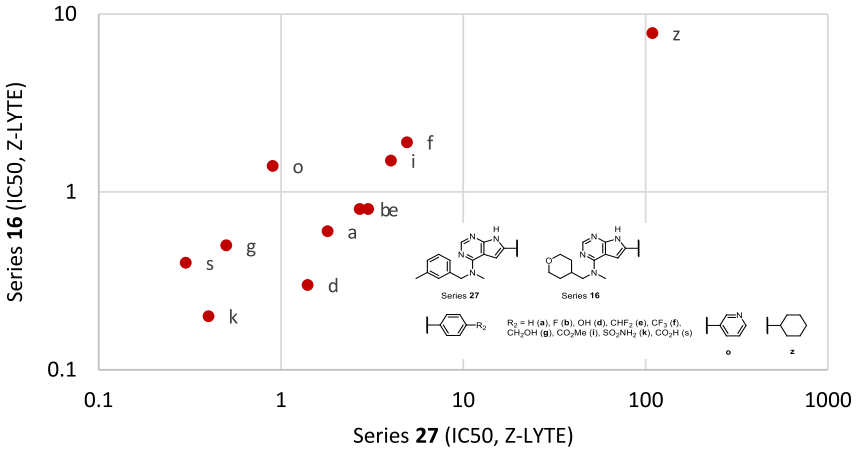

Fig. 5. Comparison of CSF1R IC_{50} values for 11 pairs of compounds at low ATP concentration using Z-LYTE assay. The scale is logarithmic.

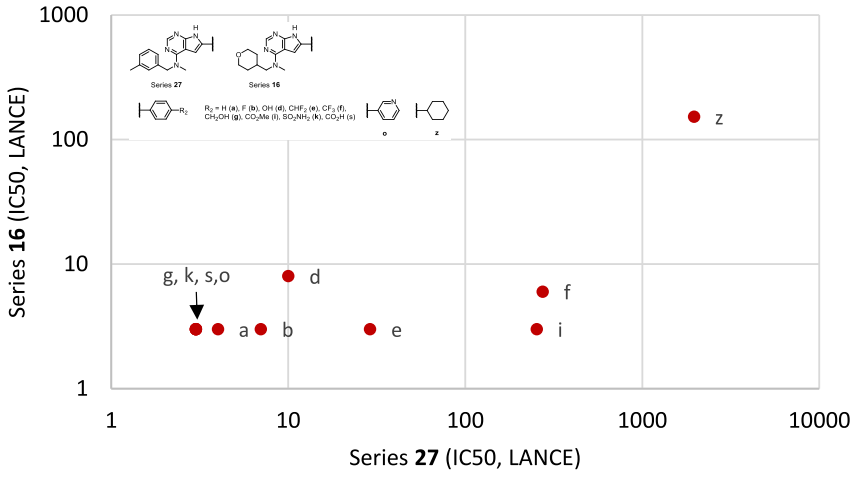

Fig. 6. Comparison of CSF1R IC_{50} values for 11 pairs of compounds at higher ATP concentration using LANCE assay. The scale is logarithmic.

Anyhow, the *para*-methoxy **16c**, *para*-hydroxyl **16d**, the oxetane **16m**, the *para*-aniline **16t** and the cyclohexene **16x** had promising IC_{50} values towards Ba/F3 cells (IC_{50}: 0.5 – 1.4 μM) and were selected for further ADME evaluation.

2.3.3. *Comparison of aromatic and THP based scaffolds*

We were also interested to see how the enzymatic activity of the THP series of compounds compared to that using an aromatic amine. Thus, eleven substitution patterns in the THP series (**16**) had also been prepared with *N*-methyl-1-(*m*-tolyl)methanamine at C-4 (scaffold **27**) [16]. We also included one new compound with a cyclohexyl at C-6 (comp. **27z**). Fig. 5 shows how the IC_{50}-values (Z–LYTE) correlates between these two series.

Overall, the THP containing series had lower IC_{50}-values, and especially so for the fluoro-containing compounds and the methyl ester. Only the pyridyl substituted derivative had better activity in the aromatic series. No major difference is seen for the most potent compounds, which probably hits the assay wall, the inherent limit encountered when reaching half the kinase test concentration. Fig. 6 shows the same plot based on assays with higher ATP concentration (LANCE, 25 μM ATP), where the assay wall is around 3 nM. Four of the pairs of derivatives had comparable IC_{50}-values (CH_2OH, SO_2NH_2, CO_2H and 3-pyridyl) in the two series. A modest drop in IC_{50} was noted for **27b** and **27d** as compared to **16b**/**16d**, while the fluorinated derivative **27e**, **27f**, the ester **27i** and the cyclopropyl **27y** lost potency compared to the corresponding THP derivatives. On average compound based on the THP unit is more tolerant to higher ATP concentration than the aromatic structures **27**.

We also compared the measured solubility of the eleven pairs of aromatic and THP based CSF1R inhibitors. By switching from scaffold **27** to **16**, the solubility increased for nine of the eleven derivatives by at least one order of magnitude. The increase in solubility was less for the difluoro and trifluoro derivatives **16e** and **16f** (see supporting information Table S4).

The Ba/F3 cellular assay using IL-3 was used as a toxicity measurement for the compounds. Table S5 in the Supporting information compares the cellular toxicity in the two series of compounds. Although the number of compounds compared is limited, it appears that scaffold **27** causes higher toxicity (4 out of 11 showed cellular toxicity) than for **16** (1 out of 11). The origin of the toxicity is currently not identified.

2.3.4. *ADME profiling of most promising THP compounds*

Five selected compounds were evaluated for their metabolic stability (clearance) towards mice liver microsomes (MLM) and human liver microsomes (HLM), mice phase II metabolism, mice protein binding and the apparent permeability coefficient (P_{app}) by a MDCK permeability

Table 4
In vivo ADME profiling of selected compounds.

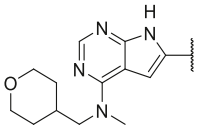

Comp.	Substituent	Sol.[a]	MLM[b]	HLM[c]	Phase II mouse[d]	PPB [%][e]	P_{app}, A-B[f]	P_{app}, B-A[f]
16c	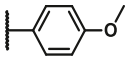	33	289	ND[g]	>99	ND[g]	ND[g]	ND[g]
16d	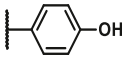	25	52	11	92	89	27	39
16m	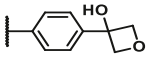	9	36	11	ND	75	0.1	7
16t	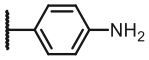	12	22	14	>99	76	38	27
16x		38	347	69	95	97	18	7
PLX3397		21	41	12	69	99	4.5	1.5

[a] Kinetic solubility (μM) determined spectrophotometrically at pH 7.4 in HEPES buffer.
[b] MLM: *in vitro* intrinsic clearance of compounds in mouse liver microsome (μl/min/mg) – Phase I.
[c] HLM*: In vitro* intrinsic clearance of compounds in human liver microsome (μl/min/mg) – Phase I.
[d] Mouse microsomal stability, phase II metabolism, remaining compound (%) at 5 mM concentration.
[e] Mouse plasma protein binding, fraction bound.
[f] Apparent permeability coefficient (P_{app}) measured by cell monolayer of Madin Darby canine kidney (MDCK) cells in the A-B and B-A directions.
[g] ND = Not determined.

assay. The data is compared with results for PLX3397 in Table 4.

Firstly, the methoxy analogue **16c** and the cyclohexene derivative **16x**, had a high clearance in MLM, excluding them for *in vivo* experimentation. The phenolic derivative **16d** appeared more stable and had good permeability as measured by MDCK. The oxetane based analogue **16m** had metabolic stability in line with that found for PLX3397. However, its permeability was low especially in the A-B direction. This was confirmed by the Caco-2 assay (efflux ratio = 40). Finally, the aniline structure **16t**, also had a metabolic stability suited for *in vivo* mice studies, and permeability values which seemed promising.

The most promising inhibitor **16t** was finally screened towards a panel of 50 kinases at 500 nM test concentrations. The inhibition profile is shown in Fig. 7 and the data is also shown in Supporting Information File, Table S2. The compound proved to be highly selective for CSF1R with respect to the other PDGFR kinase members (FLT3, KIT and PDGFRB), but also showed relative high inhibition of EPHA2, ABL2 and YES1. Calculation of the selectivity score (S-score) [32] using 50% and 30% inhibition as threshold gave S-scores of 0.16 and 0.36, respectively. Although, the solubility and the cellular activity was lower than that of PLX3397, this inhibitor might be a hit for progressing this series of compounds.

3. Conclusion

In medicinal chemistry, a transition from carbon aromatic structures to sp^3-hybridised units, can be beneficial. Based on a series of pyrrolopyrimidine CSF1R inhibitors containing carbon aromatics in the 4 and 6 position, we wanted to replace these with ring systems containing more sp^3-atoms. An initial series of 7 amine variations at C-4, showed a THP containing amine to be most promising in terms of enzymatic inhibitory activity and solubility. A SAR study varying the group at C-6 with aromatic and non-aromatic groups (27 examples) was undertaken. This showed most of the compounds to be highly active in enzymatic inhibition studies. The cyclohexene based **16x** and the 3,6-dihydro-2*H*-pyran derivative **16y** were exceptionally active but were indicated to be metabolically unstable. Unfortunately, the fully saturated analogues lost potency. Modelling indicates this to be caused by a somewhat strained binding conformation. Comparison of 11 pairs of inhibitors containing THP amines and benzylic amines, indicated the former class to be more active in enzymatic assays, more soluble and exhibited lower cellular toxicity. However, the excellent enzymatic inhibition data did not translate to cellular activity, which is not fully understood in every case. Five derivatives were further profiled by ADME assays, whereas the aniline derivative **16t** seemed most promising for further work. Assayed in a panel of 50 kinases, this compound is indicated to have high selectivity for CSF1R as opposed to the other PDGFR family members, but also hitting some off targets including EPHA2, ABL2 and YES1.

4. Experimental

4.1. Chemicals and analysis

Compound **1** was prepared multiple times as previously described by Aarhus et al. [15]. *N*-Methyl-1-(tetrahydro-2*H*-pyran-4-yl)methanamine was from Enamine, while 2-(tetrahydro-2*H*-pyran-4-yl)pyrrolidine was from CHEM SPACE. All other reagents, starting materials and solvents were purchased from Sigma-Aldrich and used as is. Dry solvents were collected from a Braun MB SPS-800 solvent purification system. Reactions were monitored by thin-layer chromatography (TLC) using silica-gel on aluminium plates, F254, Merck. Purification of compounds by flash column chromatography was performed on pre-packaged silica-gel cartridges obtained from Interchim (PuriFlash cartridges) or with silica-gel (40–63 mesh, 60 Å) using standard glassware. NMR spectra were recorded on a Bruker Avance III HD 400 or 600 MHz instrument in either $CDCl_3$ containing tetramethylsilane or DMSO-d_6 as solvents. ^1H and ^{13}C chemical shifts are reported in part per million (ppm) using tetramethylsilane (0.00 ppm) or residual solvent (DMSO-d_6, 2.50/39.52 ppm) as internal reference standard. Infrared absorption spectra were

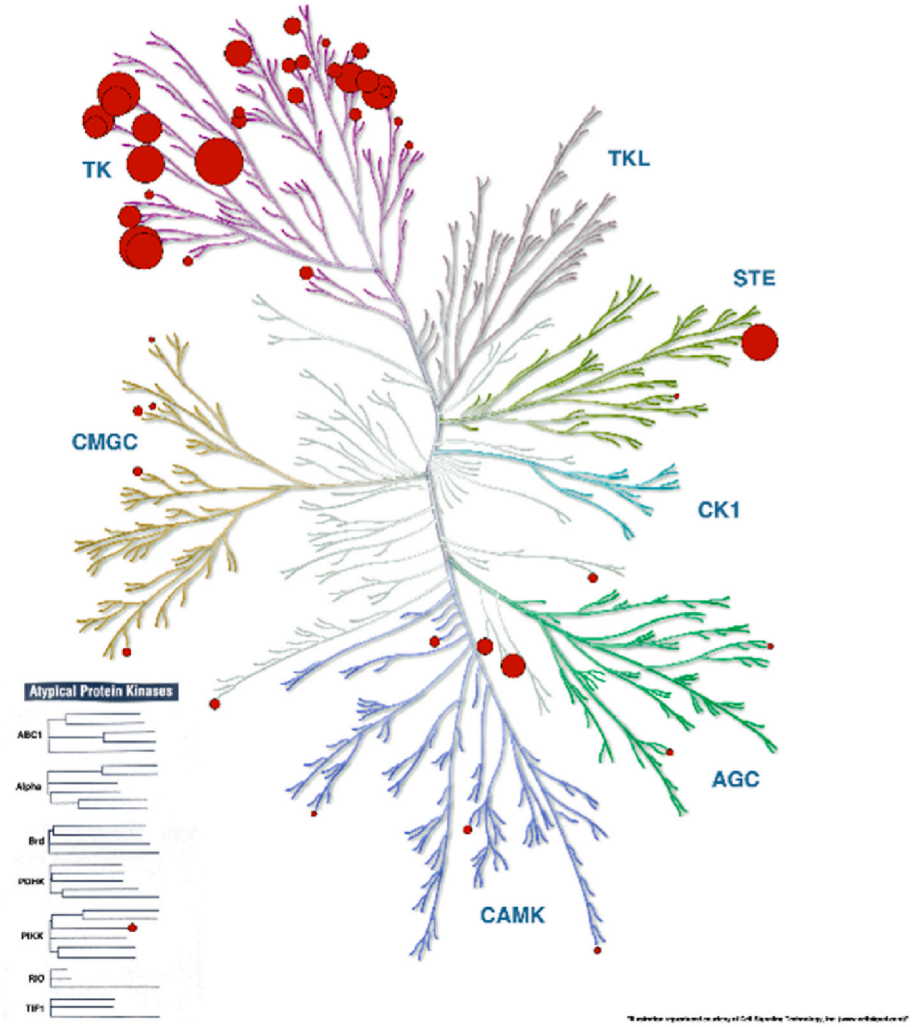

Fig. 7. Profiling of compound **16t** towards a panel of 50 kinases at 500 nM test concentration represented with a kinome tree. Larger spheres indicate higher potency. The graphic was made using the stand-alone version of Kinome Render [33].

recorded on a Thermo Nicolet Nexus FT-IR spectrometer using a Smart Endurance reflection cell. Absorption bands are reported as strong (s), medium (m) or weak (w). Accurate mass determination was performed on a Synapt G2-S Q-TOF instrument from Waters TM in either positive or negative mode. The samples were ionized with an ASAP (APCI) or ESI probe. Exact mass calculations and spectra processing was done using Waters TM Software Masslynx V4.1 SCN871. The purity of the final inhibitors was assessed on HPLC. HPLC method A: Agilent 1290-series modular HPLC instrument with a diode array detector using a C-18 Poroshell 120 (100 × 4.6 mm, 2.7 μm) column. Flow rate: 1 mL/min with a gradient elution of MeCN/H_2O. 10 % MeCN to 100 % MeCN over 20 min. The chromatograms were recorded and analysed at 254 or 320 nm and processed using Agilent ChemStation software. HPLC method B: Waters Acquity UPLC system, a Waters Acquity BEH C18 (50 × 2.1 mm, 1.7 μm) column, running at a flow rate of 0.5 mL/min. A gradient elution using MeCN/H_2O as mobile phase was performed as follows: 5 % MeCN for 0.5 min, then a linear gradient up to 95 % MeCN over 7.5 min, and finally 95 % MeCN for 1.5 min. The column was kept at a temperature of 60 °C. For each run, 5 μL of a 200 μM solution of the analyte dissolved in MeOH/H_2O (75:25 vol%) was injected. Waters MassLynx 4.1 or Agilent Chemstation was used as software.

4.2. Synthesis

4.2.1. General procedure A: amination at C-4

4-Chloro-6-iodo-7-((2-(trimethylsilyl)-ethoxy)methyl)-7*H*-pyrrolo [2,3-*d*]pyrimidine (1.00 g, 1 equiv.) was dissolved in dry *n*-BuOH or dioxane (10 mL), added the amine (1.5–3 equiv.) and optionally *N,N*-diisopropylethylamine (1.5–3 equiv.). The reaction was stirred at 100–140 °C for 4–24 h. Following evaporation of solvent, the residue was added water (20 mL) and EtOAc (50 mL). After phase separation the water phase was extracted with more EtOAc (3 × 50 mL). The combined organic phase was then dried over $MgSO_4$ and concentrated at low pressure. The products were purified by silica-gel column chromatography as specified for each compound.

4.2.2. General procedure B: Suzuki on 4-aminated compounds

The 4-amino-6-iodo-7-((2-(trimethylsilyl)-ethoxy)methyl)-7*H*-pyrrolo[2,3-*d*]pyrimidine (1.0 equiv.), aryl boronic acid or pinacol ester (1.0–1.2 equiv.), $PdCl_2$dppf (2–5 mol%) and K_2CO_3 (3.0 equiv.) were charged in an appropriate reaction vessel. The atmosphere was evacuated and back-filled with N_2 three times before adding degassed 1,4-dioxane (6 mL/mmol starting material) and degassed water (3 mL/mmol starting material). The reaction vessel was lowered into an oil-bath set at 60–80 °C and stirred vigorously. Upon reaction completion, the reaction vessel was raised from the oil-bath and allowed to cool for 5 min before the volatiles were removed by rotary evaporation. The

residue was added water (20 mL/mmol starting material) and extracted with CH_2Cl_2 (3 × 20 mL/mmol starting material). The combined organic layers were washed with brine (20 mL/mmol), dried with anhydrous Na_2SO_4 and filtered. The organic solvent was removed under reduced pressure and the crude product was purified by silica-gel column chromatography as specified for each compound.

4.2.3. General procedure C: SEM-deprotection

The SEM-protected pyrrolopyrimidine (0.2 mmol, 1 equiv.) was stirred in TFA (2 mL) and CH_2Cl_2 (10 mL) at 50 °C for 1–24 h. The reaction mixture was then concentrated in *vacuo* before it was taken up in THF (10 mL) and $NaHCO_3$ (20 mL, 25 % aqueous) and stirred for 2–24 h at 22 °C. The reaction mixture was concentrated in *vacuo*, and the crude product was purified with silica-gel column chromatography as specified for each compound. Yields in the range of 50–95 % were seen.

4.3. Compounds tested for CSF1R activity

4.3.1. N-Methyl-6-phenyl-N-((tetrahydro-2H-pyran-4-yl)methyl)-7H-pyrrolo[2,3-d]pyrimidin-4-amine (16a)

The reaction was run as described in general procedure C using **9a** (60 mg, 0.133 mmol), for 2.5 h in the first step and 16 h with THF/water/$NaHCO_3$ in the basic step. Purification by silica-gel column chromatograph (CH_2Cl_2/MeOH, 9:1, R_f = 0.50) gave 28 mg (0.088 mmol, 66 %) of a white powder, mp. > 235 °C (decomp); HPLC purity (method B): 97 %; ^{1}H NMR (600 MHz, DMSO-d_6) δ 12.13 (s, 1H), 8.11 (s, 1H), 7.88 (d, J = 8.2 Hz, 2H), 7.42 (t, J = 7.6 Hz, 2H), 7.28 (t, J = 7.4 Hz, 1H), 7.07 (s, 1H), 3.86–3.81 (m, 2H), 3.69 (d, J = 7.4 Hz, 2H), 3.40 (s, 3H), 3.28–3.21 (m, 2H), 2.07 (ddq, J = 11.4, 7.6, 3.8 Hz, 1H), 1.58–1.51 (m, 2H), 1.35–1.25 (m, 2H); ^{13}C NMR (150 MHz, DMSO-d_6) δ 156.4, 152.8, 151.1, 132.9, 131.6, 128.8 (2C), 127.2, 124.7 (2C), 103.3, 98.9, 66.8 (2C), 55.4, 38.9, 33.9, 30.3 (2C); IR (neat, cm^{-1}): 3086 (m), 2946 (m), 2914 (m), 2834 (m), 2738 (m), 1687 (m), 1566 (s), 1542 (m), 1501 (m), 1414 (m), 1321 (m), 1140 (m), 845 (m), 834 (m), 751 (m); HRMS (ASAP+, *m/z*): found 323.1875, calcd for $C_{19}H_{23}N_4O$, $[M+H]^+$, 323.187.

4.3.2. 6-(4-Fluorophenyl)-N-methyl-N-((tetrahydro-2H-pyran-4-yl)methyl)-7H-pyrrolo[2,3-d]pyrimidin-4-amine (16b)

The reaction was run as described in general procedure C using **9b** (60 mg, 0.127 mmol), for 16 h in the first step and 18 h with THF/water/$NaHCO_3$ in the basic step. Purification by silica-gel column chromatograph (CH_2Cl_2/MeOH, 9:1, R_f = 0.50) gave 42 mg (0.123 mmol, 97 %) as a white powder, mp. > 237 °C (decomp.); HPLC purity (method A): 97 %; ^{1}H NMR (600 MHz, DMSO-d_6) δ 12.12 (s, 1H), 8.11 (s, 1H), 7.94 – 7-89 (m, 2H), 7.29–7.24 (m, 2H), 7.05 (s, 1H), 3.86–3.90 (m, 2H), 3.68 (d, J = 7.4 Hz, 2H), 3.39 (s, 3H), 3.28 – 3-21 (m, 2H), 2.06 (ddq, J = 11.5, 7.7, 3.8 Hz, 1H),1.57–1.50 (m, 2H), 1.29 (qd, J = 12.2, 4.5 Hz, 2H).; ^{13}C NMR (150 MHz, DMSO-d_6) δ 161.5 (d, J = 244.7 Hz), 156.4, 152.9, 151.1, 132.0, 128.3 (d, J = 3.2 Hz), 126.72 (d, J = 8.0 Hz, 2C), 115.7 (d, J = 21.3 Hz, 2C), 103.3, 98.9, 66.8 (2C), 55.1, 38.9, 33.9, 30.3 (2C); ^{19}F NMR (565 MHz, DMSO-d_6, C_6F_6) δ −117.2; IR (neat, cm^{-1}): 3114 (m), 2933 (m), 2869 (m), 2831 (m), 1583 (m), 1568 (s), 1542 (m), 1500 (m), 1412 (m), 1141 (m), 1095 (m), 918 (m), 834 (m), 762 (m); HRMS (ASAP+, *m/z*): found 341.1776, calcd for $C_{19}H_{22}N_4OF$, $[M+H]^+$, 341.1778.

4.3.3. 6-(4-Methoxyphenyl)-N-methyl-N-((tetrahydro-2H-pyran-4-yl)methyl)-7H-pyrrolo[2,3-d]pyrimidin-4-amine (16c)

The reaction was run as described in general procedure C using **9c** (68 mg, 0.141 mmol), for 2.5 h in the first step and 18 h with THF/water/$NaHCO_3$ in the basic step. Purification by silica-gel column chromatograph (CH_2Cl_2/MeOH, 9:1, R_f = 0.37) gave 26 mg (0.0746 mmol, 53 %) as a white powder, mp. 220–224 °C; HPLC purity (method A): 99 %; ^{1}H NMR (600 MHz, DMSO-d_6) δ 12.02 (s, 1H), 8.09 (s, 1H), 7.81 (d, J = 8.8 Hz, 2H), 6.99 (d, J = 8.9 Hz, 2H), 6.93 (s, 1H), 3.86–3.81 (m, 2H), 3.79 (s, 3H), 3.68 (d, J = 7.4 Hz, 2H), 3.39 (s, 3H), 3.24 (td, J = 11.9, 1.9 Hz, 2H), 2.06 (dqt, J = 11.4, 7.5, 3.8 Hz, 1H), 1.57–1.51 (m, 2H), 1.34–1.24 (m, 2H); ^{13}C NMR (150 MHz, DMSO-d_6) δ 158.6, 156.2, 152.6, 150.6, 133.1, 126.9 (2C), 124.2, 114.2 (2C), 103.1, 97.4, 66.7 (2C), 55.3, 55.2, 38.9, 33.9, 30.3 (2C); IR (neat, cm^{-1}): 3084 (w), 2947 (m), 2918 (m), 2833 (m), 1565 (s), 1498 (s), 1439 (m), 1414 (m), 1319 (m), 1287 (m), 1250 (s), 1177 (m), 1096 (m), 1026 (m), 834 (s); HRMS (ASAP+, *m/z*): found 353.1978, calcd for $C_{20}H_{25}N_4O_2$, $[M+H]^+$, 353.1978.

4.3.4. 4-(4-(Methyl((tetrahydro-2H-pyran-4-yl)methyl)amino)-7H-pyrrolo[2,3-d]pyrimidin-6-yl)phenol (16d)

The reaction was run as described in general procedure C using **9d** (330 mg, 0.70 mmol) for 2 h in the first step and 18 h with THF/water/$NaHCO_3$ in the basic step. The reaction mixture was concentrated in *vacuo* and added 25 (mL) CH_2Cl_2 and 5 (mL) MeOH before being stirred for 2 h. The mixture was filtrated through celite and concentrated in vacuo. Purification by silica-gel chromatography (CH_2Cl_2/MeOH, 19:1, R_f = 0.45). gave 293 mg (0.62 mmol, 90 %) of a white solid, mp. 241–243 °C (decomp); HPLC purity (method A): 98 %; ^{1}H NMR (600 MHz, DMSO-d_6) δ 11.93 (s, 1H), 9.58 (s, 1H), 8.07 (s, 1H), 7.71–7.66 (m, 2H), 6.84 (s, 1H), 6.83–6.78 (m, 2H), 3.84–3.81 (m, 2H), 3.66 (d, J = 16.7, 2H), 3.38 (s, 3H), 3.25 (td, J = 11.7, 2.1 Hz, 2H), 2.11–2.01 (m, 1H), 1.54–1.51 (m, 2H), 1.30–1.24 (m, 2H); ^{13}C NMR (151 MHz, DMSO-d_6) δ 156.9, 156.1, 152.6, 150.5, 133.6, 126.2 (2C), 122.7, 115.6 (2C), 103.3, 96.7, 66.8 (2C), 55.3, 38.8, 34.0, 30.3 (2C); IR (neat, cm^{-1}): 3107 (w), 2941 (w), 2876 (w), 1735 (s), 1664 (s) 1570 (s), 1405 (m), 1207 (m), 1151 (m), 862 (m); HRMS (ASAP+, *m/z*): found 339.1823, calcd for $C_{19}H_{23}N_4O_2$, $[M+H]^+$, 339.1821.

4.3.5. 6-(4-(Difluoromethyl)phenyl)-N-methyl-N-((tetrahydro-2H-pyran-4-yl)methyl)-7H-pyrrolo[2,3-d]pyrimidin-4-amine (16e)

The reaction was run as described in general procedure C using **9e** (103 mg, 0.205 mmol), for 2.5 h in the first step and 16 h with THF/water/$NaHCO_3$ in the basic step. Purification by silica-gel column chromatograph (CH_2Cl_2/MeOH, 9:1, R_f = 0.53) gave 61 mg (0.163 mmol, 80 %) of a yellow solid; mp. > 235 (decomp); HPLC purity (method A): 97 %; ^{1}H NMR (600 MHz, DMSO-d_6) d 12.23 (s, 1H), 8.13 (s, 1H), 8.02 (d, J = 8.1 Hz, 2H), 7.61 (d, J = 7.9 Hz, 2H), 7.21 (s, 1H), 7.04 (t, J = 56.4 Hz, 1H), 3.86–3.80 (m, 2H), 3.70 (d, J = 7.4 Hz, 2H), 3.41 (s, 3H), 3.25 (td, J = 11.7, 2.1 Hz, 2H), 2.10–2.03 (m, 1H), 1.57–1.51 (m, 2H), 1.30 (qd, J = 12.3, 4.5 Hz, 2H); ^{13}C NMR (150 MHz, DMSO-d_6) d 156.6, 153.1, 151.5, 134.1, 132.5 (t, J = 21.9 Hz), 131.8, 126.2 (t, J = 6.0 Hz, 2C), 124.9, 114.9 (t, J = 235.5 Hz, 2C), 103.3, 100.4, 66.(2C), 55.3, 39.0, 33.9, 30.3 (2C); ^{19}F NMR (565 MHz, DMSO-d_6, C_6F_6) d −111.5; IR (neat, cm^{-1}): 3083 (w), 2926 (w), 2844 (w), 1735 (m), 1565 (s) 1547 (s), 1323 (m), 1279 (m), 1014 (s), 808 (s); HRMS (ASAP+, *m/z*): found 373.1841, calcd for $C_{20}H_{23}N_4OF_2$, $[M+H]^+$, 373.1840.

4.3.6. N-Methyl-N-((tetrahydro-2H-pyran-4-yl)methyl)-6-(4-(trifluoromethyl)phenyl)-7H-pyrrolo[2,3-d]pyrimidin-4-amine (16f)

The reaction was run as described in general procedure C using **9f** (118 mg, 0.227 mmol), for 2.5 h in the first step and 16 h with THF/water/$NaHCO_3$ in the basic step. Purification by silica-gel column chromatograph (CH_2Cl_2/MeOH, 9:1, R_f = 0.43) gave 56 mg (0.143 mmol, 63 %) of a white powder; mp. 261–266 °C; HPLC purity (method A): 99 %; ^{1}H NMR (600 MHz, DMSO-d_6) δ 12.31 (s, 1H), 8.14 (s, 1H), 8.10 (d, J = 8.1 Hz, 2H), 7.77 (d, J = 8.2 Hz, 2H), 7.29 (s, 1H), 3.86–3.80 (m, 2H), 3.71 (d, J = 7.4 Hz, 2H), 3.42 (s, 3H), 3.25 (td, J = 11.7, 2.1 Hz, 2H), 2.12–2.02 (m, 1H), 1.57–1.51 (m, 2H), 1.36–1.24 (m, 2H); ^{13}C NMR (150 MHz, DMSO-d_6) δ 156.6, 153.2, 151.8, 135.5, 131.2, 126.9 (q, J = 31.6 Hz, 1C), 125.7 (q, J = 3.3 Hz, 2C) 125.2, 125.0, 123.4 (q, J = 271.4 Hz, 1C), 103.3, 101.3, 66.7 (2C), 55.3, 39.0, 33.9, 30.3 (2C); ^{19}F NMR (565 MHz, DMSO-d_6, C_6F_6) δ −63.1; IR (neat, cm^{-1}): 3089 (w), 2915 (w), 2843 (w), 1677 (m), 1567 (s), 1550 (s), 1322 (s), 1141 (s),

1105 (s), 841 (s), 769 (s); HRMS (ASAP+, *m/z*): found 391.1750, calcd for $C_{20}H_{22}N_4OF_3$, $[M+H]^+$, 391.1746.

4.3.7. (4-(4-(Methyl((tetrahydro-2H-pyran-4-yl)methyl)amino)-7H-pyrrolo[2,3-d]pyrimidin-6-yl)phenyl)methanol (16g)

The reaction was run as described in general procedure C using **9g** (77 mg, 0.159 mmol), for 2 h in the first step and 16 h with THF/water/$NaHCO_3$ in the basic step. Purification by silica-gel column chromatograph (CH_2Cl_2/MeOH, 100:7.5, $R_f = 0.15$) gave 43 mg (0.123 mmol, 78 %) of a colourless solid; ^{1}H NMR (400 MHz, DMSO-d_6) δ 12.08 (s, 1H), 8.10 (s, 1H), 7.86–7.80 (m, 2H), 7.39–7.32 (m, 2H), 7.04 (s, 1H), 5.20 (t, $J = 5.7$ Hz, 1H), 4.51 (d, $J = 5.7$ Hz, 2H), 3.87–3.79 (m, 2H), 3.69 (d, $J =$ 7.4 Hz, 2H), 3.40 (s, 3H), 3.30–3.19 (m, 2H), 2.11–2.01 (m, 1H), 1.57–1.50 (m, 2H), 1.37–1.22 (m, 2H); ^{13}C NMR (101 MHz, DMSO-d_6) δ 156.4, 152.8, 151.0, 141.6, 133.0, 130.1, 126.9 (2C), 124.5 (2C), 103.3, 98.6, 66.8 (2C), 62.6, 55.4, 39.0, 34.0, 30.3 (2C); HRMS (ASAP+, *m/z*): found 353.1975, calcd for $C_{20}H_{25}N_4O_2$, $[M+H]^+$, 353.1978.

4.3.8. 2-(4-(4-(Methyl((tetrahydro-2H-pyran-4-yl)methyl)amino)-7H-pyrrolo[2,3-d]pyrimidin-6-yl)phenyl)ethan-1-ol (16h)

The reaction was run as described in general procedure C using **9h** (96 mg, 0.194 mmol), for 2 h in the first step and 16 h with THF/water/$NaHCO_3$ in the basic step. Purification by silica-gel column chromatograph (CH_2Cl_2/MeOH, 95:5 to 97:3, $R_f = 0.17$) gave 64 mg (0.174 mmol, 89 %) of a white powder, HPLC purity (method A): 99 %; ^{1}H NMR (600 MHz, DMSO-d_6) δ 12.06 (s, 1H), 8.09 (s, 1H), 7.80–7.75 (m, 2H), 7.28–7.24 (m, 2H), 7.00 (s, 1H), 4.66 (t, $J = 5.2$ Hz, 1H), 3.86–3.80 (m, 2H), 3.68 (d, $J = 7.4$ Hz, 2H), 3.62 (td, $J = 7.0$, 5.1 Hz, 2H), 3.39 (s, 3H), 3.28–3.21 (m, 2H), 2.73 (t, $J = 7.0$ Hz, 2H), 2.11–2.01 (m, 1H), 1.57–1.51 (m, 2H), 1.34–1.22 (m, 2H); ^{13}C NMR (151 MHz, DMSO-d_6) δ 156.3, 152.7, 150.9, 138.8, 133.1, 129.3 (3C), 124.6 (2C), 103.3, 98.3, 66.8 (2C), 62.1, 55.4, 38.9, 38.7, 34.0, 30.3 (2C); IR (neat, cm^{-1}): 3118 (w, br), 2949 (w), 2907 (w), 2836 (w), 1572 (s), 1513 (s) 1404 (s), 1298 (m), 1045 (m), 760 (s); HRMS (ESI+, *m/z*): found 367.2136, calcd for $C_{21}H_{27}N_4O_2$, $[M+H]^+$, 367.2134.

4.3.9. Methyl-4-(4-(methyl((tetrahydro-2H-pyran-4-yl)methyl)amino)-7H-pyrrolo[2,3-d]pyrimidin-6-yl)benzoate (16i)

The reaction was run as described in general procedure C using **9i** (142 mg, 0.227 mmol), for 3.5 h in the first step and 5 h with THF/water/$NaHCO_3$ in the basic step. Purification by silica-gel column chromatograph (CH_2Cl_2/MeOH, 9:1, $R_f = 0.32$) gave 101 mg (0.256 mmol, 96 %) as a white powder, mp. > 238 °C (decomp.); HPLC purity (method A): 97 %; ^{1}H NMR (600 MHz, DMSO-d_6) δ 12.29 (s, 1H), 8.13 (s, 1H), 8.03 (d, $J = 8.6$ Hz, 2H), 7.98 (d, $J = 8.6$ Hz, 2H), 7.29 (s, 1H), 3.86 (s, 3H), 3.86–3.81 (m, 2H), 3.70 (d, $J = 7.4$ Hz, 2H), 3.42 (s, 3H), 3.28–3.22 (m, 2H), 2.12–2.01 (m, 1H), 1.57–1.51 (m, 2H), 1.35–1.25 (m, 2H); ^{13}C NMR (150 MHz, DMSO-d_6) δ 165.9, 156.6, 153.2, 151.7, 136.0, 131.5, 129.6 (2C), 127.6, 124.5 (2C), 103.4, 101.5, 66.8 (2C), 55.3, 52.1, 39.0, 33.9, 30.3 (2C); IR (neat, *cm^{-1}*): 3124 (w), 2949 (m), 2917 (m), 2838 (m), 1707 (s), 1668 (m), 1571 (s), 1547 (w), 1432 (w), 1416 (w), 1276 (m), 1194 (m), 1141 (m), 1105, 1095 (m), 1080 (m), 799 (m); HRMS (ASAP+, *m/z*): found 381.1927, calcd for $C_{21}H_{25}N_4O_3$, $[M+H]^+$, 381,1926.

4.3.10. N-Methyl-6-(4-nitrophenyl)-N-((tetrahydro-2H-pyran-4-yl)methyl)-7H-pyrrolo[2,3-d]pyrimidin-4-amine (16j)

The reaction was run as described in general procedure C using **9j** (137 mg, 0.275 mmol), for 3 h in the first step and 18 h with THF/water/$NaHCO_3$ in the basic step. The crude product was purified by silica-gel column chromatography (CH_2Cl_2/MeOH, 9:1, $R_f = 0.32$). This gave 89 mg (0.242 mmol, 88 %) as an orange powder, mp. > 282.0 °C (decomp.); HPLC purity (method A): 98 %; ^{1}H NMR (600 MHz, DMSO-d_6) δ 12.42 (s, 1H), 8.26 (d, $J = 9.0$ Hz, 2H), 8.17–8.14 (m, 3H), 7.43 (s, 1H), 3.87–3.80 (m, 2H), 3.71 (d, $J = 7.4$ Hz, 2H), 3.43 (s, 3H), 3.25 (td, $J = 11.7$, 2.1 Hz, 2H), 2.07 (dqt, $J = 11.3$, 7.4, 3.7 Hz, 1H), 1.57–1.51 (m, 2H), 1.30 (qd, $J = 12.6$, 4.6 Hz, 2H); ^{13}C NMR (150 MHz, DMSO-d_6) δ 156.7, 153.6, 152.3, 145.6, 138.0, 130.6, 125.1 (2C), 124.2 (2C), 103.6, 103.3, 66.7 (2C), 55.4, 38.9, 33.8, 30.3 (2C); IR (neat, *cm^{-1}*): 3094 (w), 2913 (w), 2846 (w), 1571 (s), 1507 (s), 1327 (s), 1092 (m), 845 (m), 746 (m). HRMS (ASAP+, *m/z*): found 368.1727, calcd for $C_{19}H_{22}N_5O_3$, $[M+H]^+$, 368.1723.

4.3.11. 4-(4-(Methyl((tetrahydro-2H-pyran-4-yl)methyl)amino)-7H-pyrrolo[2,3-d]pyrimidin-6-yl)benzenesulfonamide (16k)

The reaction was run as described in general procedure C using **9k** (121 mg, 0.227 mmol), for 2.5 h in the first step and 16 h with THF/water/$NaHCO_3$ in the basic step. Purification by silica-gel column chromatograph (CH_2Cl_2/MeOH, 9:1, $R_f = 0.26$) gave 86 mg (0.214 mmol, 94 %) of a white powder; mp. >235 °C (decomp); HPLC purity (method A): 96 %; ^{1}H NMR (600 MHz, DMSO-d_6) δ 12.27 (s, 1H), 8.14 (s, 1H), 8.06 (d, $J = 8.6$ Hz, 2H), 7.83 (d, $J = 8.6$ Hz, 2H), 7.35 (s, 2H), 7.27 (s, 1H), 3.86–3.80 (m, 2H), 3.70 (d, $J = 7.4$ Hz, 2H), 3.42 (s, 3H), 3.25 (td, $J = 11.7$, 2.1 Hz, 2H), 2.06 (dqt, $J = 11.1$, 7.4, 3.4 Hz, 1H), 1.57–1.51 (m, 2H), 1.31 (m, 2H); ^{13}C NMR (150 MHz, DMSO-d_6) δ 156.6, 153.2, 151.7, 142.1, 134.7, 131.4, 126.2 (2C), 124.7 (2C), 103.4, 101.2, 66.8 (2C), 55.3, 39.0, 33.9, 30.2 (2C); IR (neat, *cm^{-1}*): 3309 (m), 3211 (m), 3100 (m), 2920 (m), 2849 (m), 1694 (w), 1571 (s), 1543 (m), 1340 (m), 1325 (m), 1161 (s), 1087 (m), 767 (m), 703 (m), 541 (w); HRMS (ASAP+, *m/z*): found 402.1602, calcd for $C_{19}H_{24}N_5O_3S$, $[M+H]^+$, 402.1600.

4.3.12. N-Methyl-6-(4-(morpholinomethyl)phenyl)-N-((tetrahydro-2H-pyran-4-yl)methyl)-7H-pyrrolo[2,3-d]pyrimidin-4-amine (16l)

The reaction was run as described in general procedure C using **9l** (73 mg, 0.132 mmol), for 2 h in the first step and 16 h with THF/water/$NaHCO_3$ in the basic step. Purification by silica-gel column chromatograph (CH_2Cl_2/MeOH, 95:5) gave 50 mg (0.119 mmol, 90 %) of a colourless solid. ^{1}H NMR (600 MHz, DMSO-d_6) δ 12.08 (s, 1H), 8.10 (s, 1H), 7.85–7.80 (m, 2H), 7.36–7.32 (m, 2H), 7.03 (s, 1H), 3.86–3.80 (m, 2H), 3.69 (d, $J = 7.4$ Hz, 2H), 3.60–3.55 (m, 4H), 3.47 (s, 2H), 3.39 (s, 3H), 3.28–3.21 (m, 2H), 2.38–2.34 (m, 4H), 2.11–2.02 (m, 1H), 1.57–1.51 (m, 2H), 1.34–1.25 (m, 2H); ^{13}C NMR (151 MHz, DMSO-d_6) δ 156.4, 152.8, 151.0, 136.9, 132.9, 130.4, 129.4 (2C), 124.6 (2C), 103.3, 98.7, 66.8 (2C), 66.2 (2C), 62.1, 55.4, 53.2 (2C), 38.9, 34.0, 30.3 (2C); IR (neat, *cm^{-1}*): 3118 (w), 2917 (w), 2847 (m), 2806 (m), 1568 (s), 1503 (m), 1320 (m), 1117 (m), 1016(m), 821(s), 769 (s), 533 (m); HRMS (ASAP+, *m/z*): found 422.2549, calcd for $C_{24}H_{32}N_5O_2$, $[M+H]^+$, 422.2556.

4.3.13. 3-(4-(4-(Methyl((tetrahydro-2H-pyran-4-yl)methyl)amino)-7H-pyrrolo[2,3-d]pyrimidin-6-yl)phenyl)oxetan-3-ol (16 m)

The compound was made as described in general procedure C starting with **9m** (171 mg, 0.325 mmol). The acidic step was run for 3.5 h, while the basic step took 11 h. Purification by gradient silica-gel column chromatography (CH_2Cl_2/MeOH, 95:5 to 90:10, $R_f = 0.28$) gave 100 mg (0.252 mmol, 78 %) as a white solid, mp. 256–260 °C (decomp.); HPLC purity (method A): 99 %; ^{1}H NMR (600 MHz, DMSO-d_6) δ 12.14 (s, 1H), 8.11 (s, 1H), 7.91 (d, $J = 8.6$ Hz, 2H), 7.63 (d, $J = 8.6$ Hz, 2H), 7.08 (s, 1H), 6.37 (s, 1H), 4.78 (d, $J = 6.7$ Hz, 2H), 4.71 (d, $J = 6.8$ Hz, 2H), 3.87–3.79 (m, 2H), 3.69 (d, $J = 7.5$ Hz, 2H), 3.40 (s, 3H), 3.30–3.19 (, 2H), 2.07(ddt, $J = 10.9$, 7.1, 3.4 Hz, 1H), 1H), 1.54 (m, 2H), 1.37–1.20 (m, 2H); ^{13}C NMR (150 MHz, DMSO-d_6) δ 156.4, 152.8, 151.1, 143.0, 132.7, 130.4, 125.0 (2C), 124.5 (2C), 103.3, 98.9, 85.1 (2C), 73.9, 66.7 (2C), 55.3, 38.9, 33.9, 30.3 (2C), signal at 38.9 in DMSO peak - found from HSQC and HMBC; IR (neat, cm-1): 3343 (br, m), 2847 (m), 1568 (s), 1410 (s), 971 (s), 847 (s); HRMS (ES+, *m/z*): found 395.2085, calcd. $C_{22}H_{27}N_4O_3$, $[M+H]^+$, 395.2083.

4.3.14. N-Methyl-6-(pyridin-4-yl)-N-((tetrahydro-2H-pyran-4-yl)methyl)-7H-pyrrolo[2,3-d]pyrimidin-4-amine (16n)

Compound **9n** (137 mg, 0.303 mmol) was stirred in TFA (1.5 mL)

and CH_2Cl_2 (6.0 mL) at 50 °C for 3 h. The reaction mixture was concentrated in *vacuo* and then stirred in THF (7.5 mL) and $NaHCO_3$ (7.5 mL) over night at room temperature. The reaction mixture was concentrated in *vacuo* before it was stirred with CH_2Cl_2/MeOH (4:1, 50 mL) and filtered through celite. The reaction mixture was concentrated in *vacuo*. The crude product was purified by silica-gel column chromatography (CH_2Cl_2/MeOH, 9:1, R_f = 0.19). This gave 96 mg, (0.298 mmol, 97 %) of a white powder; mp. > 295.7 °C (decomp); HPLC purity (method A): 98 %; ^{1}H NMR (600 MHz, DMSO-d_6) δ 12.37 (s, 1H), 8.57 (d, J = 5.4, 2H), 8.15 (s, 1H), 7.86 (d, *J* = 5.4 Hz, 2H), 7.41 (s, 1H), 3.86–3.80 (m, 2H), 3.71 (d, *J* = 7.4 Hz, 2H), 3.42 (s, 3H), 3.25 (td, *J* = 11.7, 2.1 Hz, 2H), 2.11–2.04 (m, 1H), 1.56–1.50 (m, 2H), 1.30 (m, 2H); ^{13}C NMR (150 MHz, DMSO-d_6) δ 156.7, 153.3, 152.1, 150.1 (2C), 138.5, 130.0, 118.6 (2C), 103.3, 102.4, 66.7 (2C), 55.3, 38.9, 33.8, 30.3 (2C); IR (neat, cm^{-1}): 3105 (w), 2917 (w), 2848 (w), 1674 (m), 1568 (s), 1415 (m), 1330 (m), 1181 (m), 1141 (m), 801 (m); HRMS (ASAP+, *m/z*): found 324.1826 calcd for $C_{18}H_{22}N_5O$, $[M+H]^+$, 324.1824.

4.3.15. N-Methyl-6-(pyridin-3-yl)-N-((tetrahydro-2H-pyran-4-yl)methyl)-7H-pyrrolo[2,3-d]pyrimidin-4-amine (16o)

The reaction was run as described in general procedure C using **9o** (180 mg, 0.397 mmol), for 3.5 h in the first step and 18 h with THF/water/$NaHCO_3$ in the basic step. Purification by silica-gel column chromatograph (CH_2Cl_2/MeOH, 9:1, R_f = 0.52) gave 89 mg (0.276 mmol, 70 %) of a white powder, mp. 233–235 °C; HPLC purity (method A): 99 %; ^{1}H NMR (600 MHz, DMSO-d_6) δ 12.27 (s, 1H), 9.14–9.10 (m, 1H), 8.47 (dd, *J* = 4.7, 1.6 Hz, 1H), 8.27–8.18 (m, 1H), 8.13 (s, 1H), 7.44 (ddd, *J* = 8.0, 4.8, 0.9 Hz, 1H), 7.24 (s, 1H), 3.86–3.80 (m, 2H), 3.70 (d, *J* = 7.4 Hz, 2H), 3.41 (s, 3H), 3.25 (td, *J* = 11.7, 2.1 Hz, 2H), 2.10–2.03 (m, 1H), 1.57–1.51 (m, 2H), 1.30 (qd, *J* = 12.3, 4.5 Hz, 2H); ^{13}C NMR (150 MHz, DMSO-d_6) δ 157.0, 153.6, 151.9, 148.4, 146.5, 132.0, 130.3, 128.0, 124.2, 103.7, 100.8, 67.2 (2C), 55.8, 40.5, 34.4, 30.7 (2C); IR (neat, cm^{-1}): 3095 (m), 2946 (m), 2912 (m), 2745 (m), 1564 (s), 1538 (w), 1512 (m), 1424 (m), 1410 (m), 1331 (m), 1317 (m), 1298 (w), 1092 (w), 844 (m), 759 (m); HRMS (ASAP+, *m/z*): found 324.1825, calcd for $C_{18}H_{22}N_5O$, $[M+H]^+$, 324.1824.

4.3.16. (3-(4-(Methyl((tetrahydro-2H-pyran-4-yl)methyl)amino)-7H-pyrrolo[2,3-d]pyrimidin-6-yl)phenyl)methanol (16p)

The reaction was run as described in general procedure C using **9p** (80 mg, 0.169 mmol), for 2.5 h in the first step and 16 h with THF/water/$NaHCO_3$ in the basic step. Purification by silica-gel column chromatograph (CH_2Cl_2/MeOH, 9:1, R_f = 0.18) gave 51 mg (0.144 mmol, 85 %) of a white powder; mp. > 229 °C (decomp); HPLC purity (method A): 98 %; ^{1}H NMR (600 MHz, DMSO-d_6) δ 12.10 (s, 1H), 8.10 (s, 1H), 7.84–7.80 (m, 1H), 7.76–7.71 (ap. d, *J* = 7.2 Hz, 1H), 7.38 (t, *J* = 7.7 Hz, 1H), 7.25 (d, *J* = 6.8 Hz, 1H), 7.05 (ap s, 1H), 5.23 (t, *J* = 5.7 Hz, 1H), 4.54 (d, *J* = 5.7 Hz, 2H), 3.87–3.81 (m, 2H), 3.69 (d, *J* = 7.4 Hz, 2H), 3.41 (s, 3H), 3.25 (td, *J* = 11.7, 2.1 Hz, 2H), 2.12–2.01 (m, 1H), 1.57–1.51 (m, 2H), 1.27 (dd, *J* = 12.5, 4.0 Hz, 2H); ^{13}C NMR (150 MHz, DMSO-d_6) δ 156.4, 152.8, 151.1, 143.1, 133.1, 131.3, 128.6, 125.5, 123.1, 122.9, 103.3, 98.8, 66.7 (2C), 62.9, 55.3, 38.9, 33.9, 30.3 (2C); IR (neat, cm^{-1}): 3426 (m), 3184 (m), 3103 (m), 2913 (m), 2843 (m), 2737 (m), 1733 (w), 1568 (s), 1539 (m), 1514 (m), 1437 (m), 1410 (m), 1318 (m), 1301 (m), 758 (m); HRMS (ASAP+, *m/z*): found 353.1980, calcd for $C_{20}H_{25}N_4O_2$, $[M+H]^+$, 353.1978.

4.3.17. Methyl 3-(4-(methyl((tetrahydro-2H-pyran-4-yl)methyl)amino)-7H-pyrrolo[2,3-d]pyrimidin-6-yl)benzoate (16q)

The reaction was run as described in general procedure C using **9q** (150 mg, 0.285 mmol), for 2.5 h in the first step and 16 h with THF/water/$NaHCO_3$ in the basic step. Purification by silica-gel column chromatograph (CH_2Cl_2/MeOH, 9:1, R_f = 0.43) gave 69 mg (0.182 mmol, 64 %) of a white powder, mp. 206–211 °C; HPLC purity (method A): 99 %; ^{1}H NMR (600 MHz, DMSO-d_6) δ 12.29 (s, 1H), 8.48–8.44 (m, 1H), 8.16–8.13 (m, 1H), 8.12 (s, 1H), 7.87–8.83 (m, 1H), 7.57 (t, *J* = 7.8 Hz, 1H), 7.18 (d, *J* = 1.2 Hz, 1H), 3.90 (s, 3H), 3.87–3.81 (m, 2H), 3.70 (d, *J* = 7.4 Hz, 2H), 3.42 (s, 3H), 3.25 (td, *J* = 11.7, 2.1 Hz, 2H), 2.10–2.01 (m, 1H), 1.56–1.51 (m, 2H), 1.30 (m, 2H); ^{13}C NMR (150 MHz, DMSO-d_6) δ 166.2, 156.6, 153.1, 151.4, 132.2, 131.8, 130.4, 129.3 (2C), 127.7, 125.2, 103.3, 100.0, 66.8 (2C), 55.3, 52.3, 38.9, 33.9, 30.3 (2C); IR (neat, cm^{-1}): 3086 (m), 2924 (m), 2840 (m), 1710 (s), 1571 (s), 1536 (w), 1512 (m), 1432 (w), 1329 (m), 1289 (m), 1256 (s), 1081 (m), 968 (m), 846 (m), 789 (m), 747 (s); HRMS (ASAP+, *m/z*): found 381.1924, calcd for $C_{21}H_{25}N_4O_3$, $[M+H]^+$, 381.1927.

4.3.18. N-Methyl-6-(3-nitrophenyl)-N-((tetrahydro-2H-pyran-4-yl)methyl)-7H-pyrrolo[2,3-d]pyrimidin-4-amine (16r)

The reaction was run as described in general procedure C using **9r** (420 mg, 0.844 mmol), for 2.5 h in the first step and 18 h with THF/water/$NaHCO_3$ in the basic step. The crude product was purified by silica-gel column chromatography (CH_2Cl_2/MeOH, 9:1, R_f = 0.27). This gave 278 mg (0.711 mmol, 84 %) as a yellow powder, mp. > 248 °C (decomposed); HPLC purity (method A): 98 %; ^{1}H NMR (600 MHz, DMSO-d_6) δ 12.38 (s, 1H), 8.75 (t, *J* = 2.0 Hz, 1H), 8.33–8.30 (m, 1H), 8.12 (s, 1H), 8.08 (m, 1H), 7.71 (t, *J* = 8.0 Hz, 1H), 7.38 (s, 1H), 3.86–3.80 (m, 2H), 3.71 (d, *J* = 7.4 Hz, 2H), 3.43 (s, 3H), 3.25 (td, *J* = 11.7, 2.1 Hz, 2H), 2.12–2.02 (m, 1H), 1.57–1.51 (m, 2H), 1.30 (m, 2H); ^{13} C NMR (150 MHz, DMSO-d_6) δ156.8, 153.3, 151.9, 148.7, 133.5, 131.0, 130.7, 130.4, 121.5, 119.0, 103.5, 101.6, 66.9 (2C), 55.4, 38.8, 33.9, 30.4 (2C); IR (neat, cm^{-1}): 3209 (m), 3134 (m), 2927 (m), 2835 (m), 1577 (m), 1564 (s), 1546 (m), 1524 (m), 1510 (s), 1402 (m), 1345 (m), 1285 (m), 1140 (m), 1093 (m), 1069 (m), 920 (m), 849 (m), 779 (s), 737 (s), 690 (m); HRMS (ASAP+, *m/z*): found 368.1725, calcd for $C_{19}H_{22}N_5O_3$, $[M+H]^+$, 368.1723.

4.3.19. 4-(4-(Methyl((tetrahydro-2H-pyran-4-yl)methyl)amino)-7H-pyrrolo[2,3-d]pyrimidin-6-yl)benzoic acid (16s)

The ester **16i** (95 mg, 0.249 mmol, 1 equiv.) was mixed with a LiOH solution (30 mg, 1.25 mmol, 5 eq.), MeOH (4 mL), H_2O (2 mL) and dioxane (2 mL). The solution was stirred for 64 h at room temperature. The reaction mixture was concentrated in vacuo before the residue was diluted in water (10 mL). The reaction mixture was then acidified to pH 3 with HCl (2 M, 1 mL). The solid that precipitated was isolated by filtration which gave 26 mg (0.072 mmol, 29 %) of a white powder; mp. >239 °C (decomp); HPLC purity (method A): 99 %; ^{1}H NMR (600 MHz, DMSO-d_6) δ 12.89 (s, 1H), 12.27 (s, 1H), 8.13 (s, 1H), 8.01 (d, *J* = 8.5 Hz, 2H), 7.95 (d, *J* = 8.5 Hz, 2H), 7.26 (s, 1H), 3.86–3.80 (dd, *J* = 8.3, 2.5 Hz, 2H), 3.70 (d, *J* = 7.4 Hz, 2H), 3.42 (s, 3H), 3.25 (td, *J* = 11.7, 2.1 Hz, 2H), 2.11–2.02 (m, 1H), 1.57–1.51 (m, 2H), 1.30 (qd, *J* = 12.1, 4.4 Hz, 2H); ^{13}C NMR (150 MHz, DMSO-d_6) δ 167.0, 156.6, 153.2, 151.6, 135.7, 131.8, 129.8 (2C), 128.9, 124.5 (2C), 103.4, 101.2, 66.8 (2C), 55.4, 38.9, 33.9, 30.3 (2C); IR (neat, cm^{-1}): 3485 (m), 3368 (m), 3219 (s), 2941 (m), 1672 (m), 1579 (s), 1275 (s), 1250 (s), 1222 (m), 1182 (m), 1079 (s), 983 (m), 759 (s), 730 (m); HRMS (ASAP+, *m/z*): found 367.1771, calcd for $C_{20}H_{23}N_4O_3$, $[M+H]^+$, 367.1770.

4.3.20. 6-(4-Aminophenyl)-N-methyl-N-((tetrahydro-2H-pyran-4-yl)methyl)-7H-pyrrolo[2,3-d]pyrimidin-4-amine (16t)

Compound **16j** (71 mg, 0.194 mmol), NH_4Cl (93 mg, 1.74 mmol) and iron powder (33 mg, 0.581 mmol) were dissolved in degassed EtOH (7 mL) and water (3 mL) under an N_2-atmosphere. The reaction mixture was stirred at 78 °C for 4 h. The reaction mixture was filtrated through celite and extracted with CH_2Cl_2 (50 mL) and water (2 × 50 mL). The organic phase was washed with brine (30 mL), dried over Na_2SO_4, filtrated and concentrated in *vacuo*. The crude product was purified with two rounds of silica-gel column chromatography (CH_2Cl_2/MeOH, 9:1, R_f = 0.16). This gave 16 mg (0.048 mmol, 25 %) of a yellow solid; mp. > 281 °C (decomp.); HPLC purity (method B): 97 %; ^{1}H NMR (600 MHz, DMSO-d_6) δ 11.78 (s, 1H), 8.04 (s, 1H), 7.53 (d, *J* = 8.6 Hz, 2H), 6.73 (s, 1H), 6.59 (d, *J* = 8.6 Hz, 2H), 5.26 (s, 2H), 3.86–3.80 (m, 2H), 3.66 (d, *J*

= 7.4 Hz, 2H), 3.36 (s, 3H), 3.24 (td, J = 11.7, 2.1 Hz, 2H), 2.10–2.01 (m, 1H), 1.56–1.51 (m, 2H), 1.30 (m,2H); ^{13}C NMR (150 MHz, DMSO-d_6) δ 155.9, 152.4, 150.1, 148.3, 134. 5, 125.8 (2C), 119.3, 113.9 (2C), 103.4, 95.3, 66.8 (2C), 55.3, 38.8, 34.2, 30.3 (2C); IR (neat, cm^{-1}): 3441 (w), 3119 (w), 2920 (w), 1570 (s), 1502 (m), 1427 (m), 1321 (m), 1298 (m), 782 (m); HRMS (ASAP+, *m/z*): found 338.1984, calcd for $C_{19}H_{24}N_5O$, $[M+H]^+$, 338.1981.

4.3.21. 6-(3-Aminophenyl)-N-methyl-N-((tetrahydro-2H-pyran-4-yl) methyl)-7H-pyrrolo[2,3-d]pyrimidin-4-amine (16u)

Compound **16r** (260 mg, 0.707 mmol), NH_4Cl (340 mg, 6.37 mmol) and iron powder (119 mg, 2.12 mmol) were dissolved in degassed EtOH (14 mL) and water (6 mL) under an N_2-atmosphere. The reaction mixture was stirred at 78 °C for 3 h. The reaction mixture was filtrated through celite and extracted with CH_2Cl_2 (50 mL) and water (2 × 50 mL). The organic phase was washed with brine (30 mL), dried over Na_2SO_4, filtrated and concentrated in *vacuo*. The crude product was purified with two rounds of silica-gel column chromatography (CH_2Cl_2/MeOH, 9:1, R_f = 0.26). This gave 160 mg (0.474 mmol, 67 %) of a white solid, mp. 196–201 °C; HPLC purity (method A): 99 %; ^{1}H NMR (600 MHz, DMSO-d_6) δ 11.97 (s, 1H), 8.09 (s, 1H), 7.06 (t, J = 8.0 Hz, 1H), 7.02–6.97 (m, 2H), 6.83 (s, 1H), 6.56–6.45 (m, 1H), 5.08 (s, 2H), 3.87–3.81 (m, 2H), 3.67 (d, J = 7.3 Hz, 2H), 3.38 (s, 3H), 3.25 (td, J = 11.7, 2.1 Hz, 2H), 2.13–1.98 (m, 1H), 1.57–1.51 (m, 2H), 1.29 (m, 2H); ^{13}C NMR (150 MHz, DMSO-d_6) δ 156.3, 152.6, 150.8, 148.8, 134.0, 132.0, 129.3, 113.4, 112.9, 110.2, 103.2, 97.9, 66.7 (2C), 55.4, 38.9, 33.9, 30.3 (2C); IR (neat, cm^{-1}): 3301 (m), 3172 (m), 2948 (m), 2928 (m), 2909 (m), 2835 (m), 1566 (s), 1081 (m), 850 (m), 792 (m), 782 (m), 757 (m); HRMS (ASAP+, *m/z*): found 338.1998, calcd for $C_{19}H_{24}N_5O$, $[M+H]^+$, 338.1981.

4.3.22. N-(3-(4-(Methyl((tetrahydro-2H-pyran-4-yl)methyl)amino)-7H-pyrrolo[2,3-d]pyrimidin-6-yl)phenyl)propionamide (16v)

The aniline derivative **16u** (70 mg, 0.207 mmol) was dissolved in CH_2Cl_2 (3 mL), and *N*,*N*-diisoproylethylamine (0.072 mL, 0.415 mmol) and cooled to 0 °C. Propionyl chloride (0.036 mL, 0.415 mmol) was added dropwise under nitrogen atmosphere. The reaction mixture was stirred for 2 h before the reaction was quenched with saturated $NaHCO_3$ (10 mL) and extracted with EtOAc (3 × 30 mL). The combined organic phases were dried over Na_2SO_4 and concentrated in vacuo. (CH_2Cl_2/MeOH, 9/1, R_f = 0.25). The product was purified by silica-gel column chromatography (CH_2Cl_2/MeOH, 95:5, R_f = 0.45). This gave 65 mg (0.144 mmol, 69 %) of a white powder, mp. 200–205 °C, HPLC purity (method A): 98 %; ^{1}H NMR (600 MHz, DMSO-d_6) δ 12.12 (s, 1H), 9.90 (s, 1H), 8.11 (s, 1H), 8.03 (s, 1H), 7.51 (d, J = 7.8 Hz, 1H), 7.48 (d, J = 8.5 Hz, 1H), 7.34 (t, J = 7.9 Hz, 1H), 6.88 (s, 1H), 3.87 – 3-81 (m, 2H), 3.68 (d, J = 7.4 Hz, 2H), 3.40 (s, 3H), 3.25 (td, J = 11.7, 2.1 Hz, 2H), 2.34 (m, 2H), 2.11–2.02 (m, 1H), 1.58–1.53 (m, 2H), 1.29 (m, 2H), 1.10 (m, 3H); ^{13}C NMR (150 MHz, DMSO-d_6) δ 172.1, 156.4, 152.9, 151.1, 139.7, 133.2, 132.0, 129.1, 119.6, 118.4, 115.8, 103.2, 98.7, 66.8 (2C), 55.4, 38.9, 34.0, 30.3 (2C), 29.5, 9.6; IR (neat, cm^{-1}): 3213 (m), 3053 (m), 2953 (s), 2931 (s), 2851 (s), 1734 (m), 1571 (s), 1264 (s), 1077 (s), 836 (s), 731 (s), 703 (s); HRMS (ASAP+, *m/z*): found 394.2239, calcd for $C_{22}H_{28}N_5O_2$, $[M+H]^+$, 394.2243.

4.3.23. N-(3-(4-(Methyl((tetrahydro-2H-pyran-4-yl)methyl)amino)-7H-pyrrolo[2,3-d]pyrimidin-6-yl)phenyl)acrylamide (16w)

The aniline **16u** (100 mg, 0.296 mmol) was dissolved in CH_2Cl_2 (3 mL) and *N*,*N*-diisoproylethylamine (0.129 ml, 0.741 mmol) and cooled to 0 °C. Acryloyl chloride (0.06 mL, 0.741 mmol) was added dropwise under nitrogen atmosphere. The reaction mixture was stirred for 4 h before the reaction was quenched with saturated $NaHCO_3$ (30 mL) and extracted with EtOAc (3 × 30 mL). The combined organic phases were dried over Na_2SO_4 and concentrated in *vacuo*. The crude product was purified by silica-gel column chromatography (CH_2Cl_2/MeOH, 95:5, R_f = 0.44). This gave 41 mg (0.104 mmol, 35 %) of a white powder, mp. > 288 °C (decomp); HPLC purity (method A): 99 %; ^{1}H NMR (600 MHz, DMSO-d_6) δ 12.15 (s, 1H), 10.20 (s, 1H), 8.12 (s, 1H), 8.09 (s, 2H), 7.56 (dd, J = 7.9, 1.9 Hz, 1H), 7.38 (t, J = 7.9 Hz, 1H), 6.92 (s, 1H), 6.47 (dd, J = 17.0, 10.2 Hz, 1H), 6.29 (dd, J = 17.0, 1.9 Hz, 1H), 5.78 (dd, J = 10.1, 1.9 Hz, 1H), 3.87–3.81 (m, 2H), 3.69 (d, J = 7.3 Hz, 2H), 3.41 (s, 3H), 3.25 (td, J = 11.8, 2.1 Hz, 2H), 2.11–2.03 (m, 1H), 1.58–1.53 (m, 2H), 1.30 (qd, J = 12.5, 4.5 Hz, 2H); ^{13}C NMR (150 MHz, DMSO-d_6) δ 163.3, 156.4, 152.9, 151.2, 139.4, 133.0, 132.2, 131.8, 129.3, 127.0, 120.2, 118.7, 116.2, 103.2, 98.9, 66.7 (2C), 55.4, 38.9, 33.9, 30.3 (2C); IR (neat, cm^{-1}): 3101 (w), 1667 (m), 1563 (s), 1407 (m), 1318 (m), 1236 (m), 763 (m); HRMS (ASAP+, *m/z*): found 392.2093, calcd for $C_{22}H_{26}N_5O_2$, $[M+H]^+$, 392.2087.

4.3.24. 6-(Cyclohex-1-en-1-yl)-N-methyl-N-((tetrahydro-2H-pyran-4-yl) methyl)-7H-pyrrolo [2,3-d]pyrimidin-4-amine (16x)

The reaction was run as described in general procedure C using **9x** (180 mg, 0.397 mmol), for 2 h in the first step and 16 h with THF/water/$NaHCO_3$ in the basic step. Purification by silica-gel column chromatography (CH_2Cl_2/MeOH, 19:1, R_f = 0.42) gave 93 mg (0.28 mmol, 87 %) of an off-white powder, mp. 231–235 °C; HPLC purity (method A): 98 %; ^{1}H NMR (600 MHz, DMSO-d_6) δ 11.64 (s, 1H), 8.06 (s, 1H), 6.46 (s, 1H), 6.40–6.35 (m, 1H), 3.83 (ddd, J = 11.4, 4.5, 1.8 Hz, 2H), 3.64 (d, J = 7.4 Hz, 2H), 3.33 (s, 3H), 3.24 (td, J = 11.7, 2.1 Hz, 2H), 2.40–2.33 (m, 2H), 2.21–2.14 (m, 2H), 2.09–1.99 (m, 1H), 1.74–1.67 (m, 2H), 1.64–1.57 (m, 2H), 1.55–1.49 (m, 2H), 1.32–1.22 (m, 2H); ^{13}C NMR (151 MHz, DMSO-d_6) δ 156.1, 152.5, 150.8, 134.9, 127.8, 122.6, 102.5, 97.5, 66.7 (2C), 55.3, 38.8, 34.0, 30.3 (2C), 25.0, 24.9, 22.1, 21.8; IR (neat, cm^{-1}): 3130 (w), 2980 (w), 2838 (w), 1667 (s), 1566 (s), 1506 (s), 1348 (s), 985 (s), 832 (s), 764 (s); HRMS (ASAP+, *m/z*): found 327.2189, calcd for $C_{19}H_{27}N_4O$, $[M+H]^+$, 327.2184.

4.3.25. 6-(3,6-Dihydro-2H-pyran-4-yl)-N-methyl-N-((tetrahydro-2H-pyran-4-yl)methyl)-7H-pyrrolo[2,3-d]pyrimidin-4-amine (16y)

The reaction was run as described in general procedure C using **9y** (252 mg, 0.55 mmol), for 2 h in the first step and 12 h with THF/water/$NaHCO_3$ in the basic step. Purification was by silica-gel column chromatography (CH_2Cl_2/MeOH, 10:1, R_f = 0.40). This resulted in 178 mg (0.54 mmol, 98 %) of an off-white powder, mp. 237–239 °C (decomp); HPLC purity (method A): 97 %; ^{1}H NMR (400 MHz, DMSO-d_6) δ 11.78 (s, 1H), 8.08 (s, 1H), 6.53 (d, J = 2.2 Hz, 1H), 6.37 (t, J = 3.0 Hz, 1H), 4.23 (q, J = 2.7 Hz, 2H), 3.87–3.77 (m, 4H), 3.64 (d, J = 7.3 Hz, 2H), 3.34 (s, 3H), 3.24 (td, J = 11.7, 2.0 Hz, 2H), 2.46–2.42 (m, 2H), 2.10–1.97 (m, 1H), 1.55–1.48 (m,2H), 1.34–1.19 (m, 2H); ^{13}C NMR (101 MHz, DMSO-d_6) δ 156.3, 152.7, 151.2, 133.4, 125.6, 120.8, 102.5, 98.4, 66.7 (2C), 64.7, 63.3, 55.3, 39.1, 34.0, 30.3 (2C), 25.1; IR (neat, cm^{-1}): 3189 (w), 2936 (w), 2838 (w), 1667 (s), 1582 (s), 1506 (s), 1348 (s), 941 (s), 849 (s), 764 (s); HRMS (ASAP+, *m/z*): found 329.1982, calcd for $C_{18}H_{25}N_4O_2$, $[M+H]^+$, 329.1978.

4.3.26. 6-Cyclohexyl-N-methyl-N-((tetrahydro-2H-pyran-4-yl)methyl)-7H-pyrrolo[2,3-d]pyrimidin-4-amine (16z)

The reaction was run as described in general procedure C using **9z** (80 mg, 0.174 mmol) for 3 h in the first step and 18 h with THF/water/$NaHCO_3$ in the basic step. Purification was by silica-gel chromatography (CH_2Cl_2/MeOH, 19:1, R_f = 0.28). This resulted in 51 mg (0.155 mmol, 89 %) of a white solid, mp. 231–233 °C (decomp); HPLC purity (method B): 98 %; ^{1}H NMR (600 MHz, DMSO-d_6) δ 11.45 (s, 1H), 8.02 (s, 1H), 6.20 (s, 1H), 3.83 (ddd, J = 4.5, 1.9 Hz, 2H), 3.61 (d, J = 7.4 Hz, 2H), 3.30 (s, 3H), 3.23–3.21 (m, 2H), 2.67–2.57 (m, 1H), 2.07–1.94 (m, 3H), 1.77–1.75 (dp, J = 10.5, 3.3 Hz, 2H), 1.70–1.66 (m, 2H), 1.51 (m, 2H), 1.43–1.22 (m, 6H); ^{13}C NMR (151 MHz, DMSO-d_6) δ 156.0, 151.6, 149.9, 140.4, 102.0, 95.9, 66.8 (2C), 55.3, 38.7, 36.5, 34.0, 32.1 (2C), 30.3 (2C), 25.8 (2C), 25.6; IR (neat, cm^{-1}): 3188 (w), 2916 (w), 1727 (s), 1591 (s), 1504 (s), 1348 (s), 942 (s), 849 (s), 764 (s), 648(s); HRMS (ASAP+, *m/z*): found 329.2230, calcd for $C_{19}H_{29}N_4O$, $[M+H]^+$, 329.2341.

4.3.27. N-Methyl-6-(tetrahydro-2H-pyran-4-yl)-N-((tetrahydro-2H-pyran-4-yl)methyl)-7H-pyrrolo [2,3-d]pyrimidin-4-amine (16aa)

The reaction was run as described in general procedure C using **9aa** (84 mg, 0.18 mmol) for 3 h in the first step and 16 h with THF/water/$NaHCO_3$ in the basic step. Purification was by silica-gel column chromatography (CH_2Cl_2/MeOH, 19:1, $R_f = 0.15$). This resulted in 53 mg (0.16 mmol, 88 %) of an off-white powder, mp. 338–339 °C (decomp); HPLC purity (method B) > 99 %; ^{1}H NMR (600 MHz, DMSO-d_6) δ 11.53 (s, 1H), 8.03 (s, 1H), 6.25 (d, $J = 2.1$ Hz, 1H), 3.96–3.88 (m, 2H), 3.82 (ddd, $J = 11.4$, 4.5, 1.8 Hz, 2H), 3.62 (d, $J = 7.4$ Hz, 2H), 3.42–3.40 (m, 2H), 3.31 (s, 3H), 3.22 (td, $J = 11.7$, 2.1 Hz, 2H), 2.88 (tt, $J = 11.8$, 3.8 Hz, 1H), 2.01–1.96 (m, 1H), 1.91–1.84 (m, 2H), 1.72–1.68 (m, 2H), 1.53–1.48 (m, 2H), 1.26–1.23 (m, 2H); ^{13}C NMR (151 MHz, DMSO-d_6) δ 156.1, 151.7, 150.1, 138.9, 101.9, 96.4, 66.9 (2C), 66.7 (2C), 55.3, 38.7, 34.0, 33.8, 31.8 (2C), 30.3 (2C); IR (neat, cm^{-1}): 2922 (w), 2852 (w), 1664 (s), 1564 (s), 1437 (s), 1408 (s), 1199 (s), 853 (m), 750 (s); HRMS (ASAP+, *m/z*): found 331.2140, calcd for $C_{18}H_{27}N_4O_2$, $[M+H]^+$, 331.2134.

4.3.28. N-(Cyclohexylmethyl)-N-methyl-6-phenyl-7H-pyrrolo[2,3-d] pyrimidin-4-amine (17a)

The reaction was run as described in general procedure C using **10a** (94 mg, 0.2 mmol) for 1 h in the first step and 18 h with THF/water/$NaHCO_3$ in the basic step. The reaction mixture was concentrated in *vacuo*, and added water (5 mL). The resulting precipitate was filtered and washed with *n*-pentane (5 mL). The resulting solid was purified by silica-gel column chromatography (CH_2Cl_2/MeOH, 19:1, $R_f = 0.56$). This gave 51 mg (0.16 mmol, 79 %) of a white solid, mp. 229–231 °C (decomp); HPLC purity (method B): 98 %; ^{1}H NMR (400 MHz, DMSO-d_6) δ 12.11 (s, 1H), 8.10 (s, 1H), 7.90–7.83 (m, 2H), 7.42 (t, $J = 7.8$ Hz, 2H), 7.32–7.23 (m, 1H), 7.05 (s, 1H), 3.64 (d, $J = 7.4$ Hz, 2H), 3.38 (s, 3H), 1.82 (s, 1H), 1.66 (d, $J = 10.8$ Hz, 5H), 1.25–1.11 (m, 3H), 1.00 (q, $J = 11.1$ Hz, 2H); ^{13}C NMR (101 MHz, DMSO-d_6) δ 156.5, 152.8, 151.1, 132.8, 131.6, 128.8 (2C), 127.2, 124.7 (2C), 103.2, 98.9, 55.8, 40.2, 36.5, 30.3 (2C), 26.1, 25.4 (2C); IR (neat, cm^{-1}): 3099 (m), 2935 (m), 2839 (m), 1565 (s), 1505(m), 1413 (w), 1300 (s), 1124 (m), 1095 (m), 849 (m), 768 (s); HRMS (ASAP+, *m/z*): found 321.2084, calcd for $C_{20}H_{25}N_4$, $[M+H]^+$, 321.2079.

4.3.29. 6-Phenyl-N-((tetrahydro-2H-pyran-4-yl)methyl)-7H-pyrrolo[2,3-d]pyrimidin-4-amine (18a)

The reaction was run as described in general procedure C using **11** (94 mg, 0.214 mmol) for 3 h in the first step and 18 h with THF/water/$NaHCO_3$ in the basic step. The crude product was purified with two rounds of silica-gel column chromatography (CH_2Cl_2/MeOH, 9:1, $R_f = 0.31$). This gave 39 mg (0.125 mmol, 58 %) of a white powder; HPLC purity (method A): 99 %; ^{1}H NMR (600 MHz, DMSO-d_6) δ 12.01 (s, 1H), 8.11 (s, 1H), 7.77 (d, $J = 7.4$ Hz, 2H), 7.53–7.47 (m, 1H), 7.43 (t, $J = 7.5$ Hz, 2H), 7.31–7.26 (m, 1H), 6.98 (d, $J = 2.2$ Hz, 1H), 3.89–3.82 (m, 2H), 3.38 (t, $J = 6.4$ Hz, 2H), 3.27 (td, $J = 11.7$, 2.1 Hz, 2H), 1.95–1.85 (m, 1H), 1.68–1.62 (m, 2H), 1.24 (qd, $J = 12.4$, 4.6 Hz, 2H); ^{13}C NMR (150 MHz, DMSO-d_6) δ 156.1, 151.9, 151.4, 133.2, 131.8, 128.9 (2C), 127.2, 124.5 (2C), 103.8, 95.9, 66.8 (2C), 45.7, 34.8, 30.6 (2C); IR (neat, cm^{-1}): 3339 (w), 2916 (w), 2833 (w), 1594 (s), 1455 (m), 1345 (m), 1088 (m), 750 (m); HRMS (ASAP+, *m/z*): found 309.1721 calcd for $C_{18}H_{21}N_4O$, $[M+H]^+$, 309.1715.

4.3.30. 6-Phenyl-N-(1-(tetrahydro-2H-pyran-4-yl)ethyl)-7H-pyrrolo[2,3-d]pyrimidin-4-amine (19a)

The reaction was run as described in general procedure C using **12** (112 mg, 0.247 mmol), for 4 h in the first step and 16 h with THF/water/$NaHCO_3$ in the basic step. Purification by silica-gel column chromatograph (CH_2Cl_2/MeOH, 9:1, $R_f = 0.27$) gave 76 mg (0.236 mmol, 95 %) of a white powder, mp. 243–247 °C; HPLC purity (method A): 96 %; ^{1}H NMR (600 MHz, DMSO-d_6) δ 11.98 (s, 1H), 8.09 (s, 1H), 7.77 (d, $J = 7.0$ Hz, 2H), 7.43 (t, $J = 7.8$ Hz, 2H), 7.28 (t, $J = 7.4$ Hz, 1H), 7.17 (d, $J = 8.7$ Hz, 1H), 7.04 (d, $J = 2.2$ Hz, 1H), 4.25–4.22 (m, 1H), 3.91–3.83 (m, 2H), 3.30–3.20 (m, 2H), 1.76–1.69 (m, 1H), 1.70–1.59 (m, 2H), 1.29–1.22 (m, 2H), 1.17 (d, $J = 6.7$ Hz, 3H); ^{13}C NMR (150 MHz, DMSO-d_6) δ 155.7, 151.9, 151.5, 133.1, 131.9, 128.9 (2C), 127.1, 124.4 (2C), 104.2, 96.1, 67.0 (2C), 49.1, 40.2, 29.2 (2C), 17.6; IR (neat, cm^{-1}): 3334 (w), 3111 (w), 2847 (w), 1674 (m), 1595 (s), 1454 (m), 1319 (m), 1203 (m), 1141 (m), 744 (m); HRMS (ASAP+, *m/z*): found 323.1877, calcd for $C_{19}H_{23}N_4O$, $[M+H]^+$, 323.1872.

4.3.31. 6-Phenyl-4-(2-(tetrahydro-2H-pyran-4-yl)pyrrolidin-1-yl)-7H-pyrrolo[2,3-d]pyrimidine (20a)

The reaction was run as described in general procedure C using **13** (87 mg, 0.182 mmol), for 2 h in the first step and 22 h with THF/water/$NaHCO_3$ in the basic step. Purification by silica-gel column chromatograph (CH_2Cl_2/MeOH, 9:1, $R_f = 0.23$) gave 59 mg (0.169 mmol, 93 %) of a white powder, mp. 240–250 °C; HPLC purity (method A): 97 %; ^{1}H NMR (600 MHz, DMSO) δ 12.10 (s, 1H), 8.12 (s, 1H), 7.96–7.81 (m, 2H), 7.52–7.38 (m, 2H), 7.36–7.21 (m, 1H), 7.05 (s, 1H), 4.50 (ddd, $J = 8.3$, 5.7, 2.8 Hz, 1H), 4.00–3.78 (m, 4H), 3.28–3.07 (m, 3H), 2.21 (d, $J = 7.4$ Hz, 1H), 2.09–1.79 (m, 4H), 1.58–1.31 (m, 4H); ^{13}C NMR (151 MHz, DMSO) δ 155.0, 152.4, 151.0, 132.9, 131.5, 128.5 (2C), 126.9, 124.5 (2C), 103.9, 98.2, 67.1, 66.9, 60.9, 48.6, 37.5, 29.4, 27.6, 25.5, 23.6; IR (neat, cm^{-1}): 3111 (w), 2846 (w), 1680 (m), 1562 (s), 1454 (m), 1317 (m), 1191 (m), 1138 (m), 748 (m); HRMS (ASAP+, *m/z*): found 349.2034, calcd for $C_{21}H_{25}N_5O_2$, $[M+H]^+$, 349.2028.

4.3.32. 6-Phenyl-N-(tetrahydro-2H-pyran-4-yl)-7H-pyrrolo[2,3-d] pyrimidin-4-amine (21a)

The reaction was run as described in general procedure C using **14** (89 mg, 0.208 mmol) for 3 h in the first step and 22 h with THF/water/$NaHCO_3$ in the basic step. The crude product was purified with three rounds of silica-gel column chromatography (CH_2Cl_2/MeOH, 9:1, $R_f = 0.35$. This gave 27 mg (0.091 mmol, 44 %) of a white powder, mp. > 270 °C (decomp.); HPLC purity (method A): 97 %; ^{1}H NMR (600 MHz, DMSO-d_6) δ 12.03 (s, 1H), 8.12 (s, 1H), 7.78 (d, $J = 6.9$ Hz, 2H), 7.44 (t, $J = 7.8$ Hz, 2H), 7.32 (d, $J = 7.7$ Hz, 1H), 7.29 (t, $J = 7.4$ Hz, 1H), 7.00 (d, $J = 2.2$ Hz, 1H), 4.33–4.24 (m, 1H), 3.94–3.88 (m, 2H), 3.44 (td, $J = 11.7$, 2.1 Hz, 2H), 1.94–1.88 (m, 2H), 1.57 (qd, $J = 12.2$, 4.4 Hz, 2H); ^{13}C NMR (150 MHz, DMSO-d_6) δ 155.0, 151.8, 151.4, 133.2, 131.7, 128.8 (2C), 127.1, 124.4 (2C), 103.8, 95.8, 66.2 (2C), 46.1, 32.9 (2C); IR (neat, cm^{-1}): 3132 (w), 2952 (w), 2839 (w), 1599 (s), 1471 (m), 1360 (m), 1141 (m), 904 (m), 754 (m); HRMS (ASAP+, *m/z*): found 295.1563, calcd for $C_{17}H_{19}N_4O$, $[M+H]^+$, 295.1559.

4.3.33. 4-(6-Phenyl-7H-pyrrolo [2,3-d]pyrimidin-4-yl)morpholine (22a)

Compound **15** (120 mg, 0.292 mmol) was stirred in TFA (1.5 mL) and CH_2Cl_2 (6.0 mL) at 50 °C for 3 h. The reaction mixture was concentrated in *vacuo* and then stirred in THF (7.5 mL) and $NaHCO_3$ (7.5 mL) 18h at room temperature. The reaction mixture was concentrated in *vacuo* before it was stirred with CH_2Cl_2/MeOH (4:1, 50 mL) and filtered through celite. The reaction mixture was concentrated in *vacuo*. The crude product was purified by silica-gel column chromatography (CH_2Cl_2/MeOH, 9:1, $R_f = 0.17$). This gave 70 mg (0.250 mmol, 86 %) of a white powder, mp. > 290.2 °C (decomp); HPLC purity (method B): 99 %; ^{1}H NMR (600 MHz, DMSO-d_6) δ 12.24 (s, 1H), 8.19 (s, 1H), 7.92 (d, $J = 7.0$ Hz, 2H), 7.43 (t, $J = 7.8$ Hz, 2H), 7.30 (t, $J = 7.4$ Hz, 1H), 7.19 (s, 1H), 3.91–3.86 (m, 4H), 3.77–3.73 (m, 4H); ^{13}C NMR (150 MHz, DMSO-d_6) δ 156.3, 153.3, 150.8, 133.8, 131.4, 128.8 (2C), 127.5, 124.9 (2C), 103.7, 98.2, 66.1 (2C), 45.6 (2C); IR (neat, cm^{-1}): 3102 (w), 2920 (w), 2849 (w), 1564 (s), 1435 (m), 1257 (m), 1106 (m), 1024 (m), 928 (m), 736 (m); HRMS (ASAP+, *m/z*): found 281.1407, calcd for $C_{16}H_{17}N_4O$, $[M+H]^+$, 281.1402.

4.4. Biochemical assays

4.4.1. CSF1R enzymatic inhibitory assay

The compounds were supplied in a 10 mM DMSO solution, and enzymatic CSF1R inhibition potency was determined by Invitrogen (ThermoFisher) using their Z′-LYTE® assay technology [28]. The assay is based on fluorescence resonance energy transfer (FRET). In the primary reaction, the kinase transfers the gamma-phosphate of ATP to a single tyrosine residue in a synthetic FRET-peptide. In the secondary reaction, a site-specific protease recognizes and cleaves non-phosphorylated FRET-peptides. Thus, phosphorylation of FRET-peptides suppresses cleavage by the development reagent. Cleavage disrupts FRET between the donor (i.e. coumarin) and acceptor (i.e., fluorescein) fluorophores on the FRET-peptide, whereas uncleaved, phosphorylated FRET-peptides maintain FRET. A ratiometric method, which calculates the ratio (the emission ratio) of donor emission to acceptor emission after excitation of the donor fluorophore at 400 nm, is used to quantitate inhibition. All compounds were first tested for their inhibitory activity at 500 nM in duplicates. The potency observed at 500 nM was used to set starting point of the IC_{50} titration curve, in which two levels were used 1000 or 10000 nM. The IC_{50} values reported are based on the average of at least 2 titration curves (minimum 20 data points), and were calculated from activity data with a four parameter logistic model using SigmaPlot (Windows Version 12.0 from Systat Software, Inc.) Unless stated otherwise the ATP concentration used was equal to K_M (ca 10 mM).

4.4.2. CSF1R enzymatic inhibitory assay (LANCE)

The TR-FRET-based LANCE *Ultra* assay (PerkinElmer) was used to determine IC_{50} values for various CSF1R inhibitors. Kinase activity and inhibition in this assay was measured as recommended by the manufacturer. Briefly, a specific Ultra ULight GT peptide substrate (50 nM final concentration) was allowed to get phosphorylated by CSF1R (0.5 nM final concentration) in enzymatic buffer (50 mM Hepes pH 7.5, 10 mM $MgCl_2$, 1 mM EGTA, 0.01 % Tween 20, 2 mM dithiothreitol, 1 % DMSO) containing ATP at 25 μM or 2.5 mM of the kinase for 1 h at room temperature. All compounds were tested in an 8-point dose response curve up to a final concentration of 10 μM. The compound transfer was facilitated via acoustic dispensing with the Echo 520 (Beckman Labcyte) using the Echo Dose Response software package. Subsequently, phosphorylation or inhibition was detected by addition of specific europium (Eu)-labelled anti-phospho-antibodies (2 nM), which upon binding to the phospho-peptide give rise to a FRET signal. The FRET signal was recorded in a time-resolved manner in a PerkinElmer EnVision reader. All assays were performed in a final volume of 20 μl in low volume white 384 well plates from Corning (4513). All assay data was analysed with the Quattro Workflow software package from Quattro Research.

4.4.3. Kinase panel

The compounds were supplied in a 10 mM DMSO solution, and enzymatic kinase inhibition potency was determined by ThermoFisher (Invitrogen) using their Z′-LYTE® assay technology [28], at 500 nM in duplicates.

4.4.4. Cell viability assay with Ba/F3-hCSF1R cells

Ba/F3-hCSF1R cells expressing human CSF1R were kindly provided from C. Pridens, Roslin Institute and Royal (Dick) School of Veterinary Studies, University of Edinburgh. The cells were maintained in RPMI 1640 (PAN Biotech, Cat. No.: P04-22100) supplemented with 10 % fetal calf serum, 1 % glutamine and 100 ng/mL human M-CSF (Thermo, #14-8789-80, 0.1 mg/mL) and grown at 37 °C, 5 % CO_2. For the cell viability assay, cells were seeded with a density of 1200 cells per well in 25 μL in 384-well plates (Greiner Bio-One, Frickenhausen, Germany; order no. 781080) in medium without human M-CSF. Shortly after seeding, compounds were added to each sample well by using Echo Acoustic Liquid Transfer technology (Labcyte) with 10 μM as highest concentration and 7 further 3-fold dilution steps down to 0.007 μM. Wells with cells and 0.1 % DMSO in culture medium were used as positive controls, wells with cells and 10 μM staurosporine in culture medium were used as negative controls. After a 30 min incubation time at 37 °C/5 % CO_2, the cells were stimulated by adding 10 μM human M-CSF (final conc.) to get a final assay volume of 35 μL. The cells were incubated with the compounds for 72 h at 37 °C/5 % CO_2. For measurement of cell viability 35 μL Cell Titer Glo reagent (Promega, Madison, USA; order no. G7573) - 1:2 diluted with cell culture medium was added to each well. The 384 well-plates were placed for 2 min on an orbital microplate shaker and incubated for further 10 min at room temperature to stabilize the luminescence signal. Luminescence was measured by Victor X5 Reader (PerkinElmer, USA). IC_{50} values were calculated with the software Excel Fit (IDBS, Guildford, UK) from 3-fold dilution series comprising at least 8 concentrations in duplicates.

4.5. Molecular modelling

Molecular modelling was carried out using the Maestro software package on the Schrödinger Platform (Maestro, v12.4.079, release 2020.2; Schrödinger, LLC, New York, USA). An x-ray structure of CSF1R with PDB-ID 8CGC [16] was prepared using the protein preparation wizard. Bond orders and formal charges were added for het-groups and hydrogens were added to all atoms in the system. Water molecules beyond 5 Å from het-groups were removed. An all-atom constrained minimization was performed using the OPLS3 force field. Ligands drawn in ChemBioDraw Ultra (v19.1, CambridgeSoft, PerkinElmer) were prepared using LigPrep (Schrödinger) and subsequently docked in the binding site of the energy minimized protein construct receptor grid of 8CGC [16] as defined by the co-crystallized ligand using GLIDE in SP mode [34].

CRediT authorship contribution statement

Frithjof Bjørnstad: Investigation, Writing – review & editing. **Simen Havik:** Investigation. **Thomas Ihle Aarhus:** Investigation, Methodology, Software. **Iktedar Mahdi:** Investigation. **Anke Unger:** Formal analysis, Investigation. **Peter Habenberger:** Formal analysis, Investigation. **Carsten Degenhart:** Investigation. **Jan Eickhoff:** Project administration, Resources. **Bert M. Klebl:** Project administration, Resources. **Eirik Sundby:** Conceptualization, Funding acquisition, Visualization, Writing – review & editing. **Bård Helge Hoff:** Conceptualization, Supervision, Writing – original draft, Writing – review & editing.

Declaration of competing interest

Several of the authors contributing to the work is employed at Lead Discovery Center GmbH (LDC) a translational drug discovery organization. There is no conflict of interest.

Data availability

Most of the data is included in SIF, additional data can be provided on request

Acknowledgements

The support from the Research Council of Norway to the project (Grant number: NFR 284937) and the Norwegian NMR Platform (project number 226244/F50) are highly appreciated. So is the help from the Mass Spectrometry Lab at the NV Faculty at NTNU. Hay Man Hilde Tsui is acknowledged for early work on synthesis. Roger Aarvik is thanked for technical support.

Appendix A. Supplementary data

Supplementary data to this article can be found online at https://doi.org/10.1016/j.ejmech.2023.116053.

References

[1] H. Lin, E. Lee, K. Hestir, C. Leo, M. Huang, E. Bosch, R. Halenbeck, G. Wu, A. Zhou, D. Behrens, D. Hollenbaugh, T. Linnemann, M. Qin, J. Wong, K. Chu, S. K. Doberstein, L.T. Williams, Discovery of a cytokine and its receptor by functional screening of the extracellular proteome, Science 320 (2008) 807–811, https://doi.org/10.1126/science.1154370.

[2] T.A. Wynn, A. Chawla, J.W. Pollard, Macrophage biology in development, homeostasis and disease, Nature 496 (2013) 445–455, https://doi.org/10.1038/nature12034.

[3] S. Yadav, A. Priya, D.R. Borade, R. Agrawal-Rajput, Macrophage subsets and their role: co-relation with colony-stimulating factor-1 receptor and clinical relevance, Immunol. Res. 71 (2023) 130–152, https://doi.org/10.1007/s12026-022-09330-8.

[4] A. Mantovani, P. Allavena, The interaction of anticancer therapies with tumor-associated macrophages, J. Exp. Med. 212 (2015) 435–445, https://doi.org/10.1084/jem.20150295.

[5] A. Olmos-Alonso, D. Gomez-Nicola, K. Askew, R. Mancuso, S. Sri, S.T.T. Schetters, V.H. Perry, M. Vargas-Caballero, C. Holscher, Pharmacological targeting of CSF1R inhibits microglial proliferation and prevents the progression of Alzheimer's-like pathology, Brain 139 (2016) 891–907, https://doi.org/10.1093/brain/awv379%JBrain.

[6] J. Sosna, S. Philipp, R. Albay III, J.M. Reyes-Ruiz, D. Baglietto-Vargas, F. M. LaFerla, C.G. Glabe, Early long-term administration of the CSF1R inhibitor PLX3397 ablates microglia and reduces accumulation of intraneuronal amyloid, neuritic plaque deposition and pre-fibrillar oligomers in 5XFAD mouse model of Alzheimer's disease, Mol. Neurodegener. 13 (2018) 1–11, https://doi.org/10.1186/s13024-018-0244-x.

[7] S.H. Mun, P.S.U. Park, K.-H. Park-Min, The M-CSF receptor in osteoclasts and beyond, Exp. Mol. Med. 52 (2020) 1239–1254, https://doi.org/10.1038/s12276-020-0484-z.

[8] J. Wen, S. Wang, R. Guo, D. Liu, CSF1R inhibitors are emerging immunotherapeutic drugs for cancer treatment, Eur. J. Med. Chem. 245 (2023), 114884, https://doi.org/10.1016/j.ejmech.2022.114884.

[9] W.A. Denny, J.U. Flanagan, Small-molecule CSF1R kinase inhibitors; review of patents 2015-present, Expert Opin. Ther. Pat. 31 (2021) 107–117, https://doi.org/10.1080/13543776.2021.1839414.

[10] B.D. Smith, M.D. Kaufman, S.C. Wise, Y.M. Ahn, T.M. Caldwell, C.B. Leary, W.-P. Lu, G. Tan, L. Vogeti, S. Vogeti, B.A. Wilky, L.E. Davis, M. Sharma, R. Ruiz-Soto, D.L. Flynn, Vimseltinib: a precision CSF1R therapy for tenosynovial giant cell tumors and diseases promoted by macrophages, Mol. Cancer Therapeut. 20 (2021) 2098–2109, https://doi.org/10.1158/1535-7163.Mct-21-0361.

[11] J.A. Krauser, Y. Jin, M. Walles, U. Pfaar, J. Sutton, M. Wiesmann, D. Graf, V. Pflimlin-Fritschy, T. Wolf, G. Camenisch, P. Swart, Phenotypic and metabolic investigation of a CSF-1R kinase receptor inhibitor (BLZ945) and its pharmacologically active metabolite, Xenobiotica 45 (2015) 107–123.

[12] C.L. Manthey, B.A. Moore, Y. Chen, M.J. Loza, X. Yao, H. Liu, S.M. Belkowski, H. Raymond-Parks, P.J. Dunford, F. Leon, J.E. Towne, S.E. Plevy, The CSF-1-receptor inhibitor, JNJ-40346527 (PRV-6527), reduced inflammatory macrophage recruitment to the intestinal mucosa and suppressed murine T cell mediated colitis, PLoS One 14 (2019), https://doi.org/10.1371/journal.pone.0223918.

[13] J. Guo, P.A. Marcotte, J.O. McCall, Y. Dai, L.J. Pease, M.R. Michaelides, S. K. Davidsen, K.B. Glaser, Inhibition of phosphorylation of the colony-stimulating factor-1 receptor (c-Fms) tyrosine kinase in transfected cells by ABT-869 and other tyrosine kinase inhibitors, Mol. Cancer Therapeut. 5 (2006) 1007–1013, https://doi.org/10.1158/1535-7163.Mct-05-0359.

[14] B. Czako, J.R. Marszalek, J.P. Burke, P. Mandal, P.G. Leonard, J.B. Cross, F. Mseeh, Y. Jiang, E.Q. Chang, E. Suzuki, J.J. Kovacs, N. Feng, S. Gera, A.L. Harris, Z. Liu, R. A. Mullinax, J. Pang, C.A. Parker, N.D. Spencer, S.S. Yu, Q. Wu, M.R. Tremblay, K. Mikule, K. Wilcoxen, T.P. Heffernan, G.F. Draetta, P. Jones, Discovery of IACS-9439, a potent, exquisitely selective, and orally bioavailable inhibitor of CSF1R, J. Med. Chem. 63 (2020) 9888–9911, https://doi.org/10.1021/acs.jmedchem.0c00936.

[15] T.I. Aarhus, V. Teksum, A. Unger, P. Habenberger, A. Wolf, J. Eickhoff, B. Klebl, C. Wolowczyk, G. Bjørkøy, E. Sundby, B.H. Hoff, Negishi cross-coupling in the preparation of benzyl substituted pyrrolo[2,3-d]pyrimidine based CSF1R inhibitors, Eur. J. Org. Chem. 26 (2023), e202300052, https://doi.org/10.1002/ejoc.202300052.

[16] T.I. Aarhus, F. Bjørnstad, C. Wolowczyk, K.U. Larsen, L. Rognstad, T. Leithaug, A. Unger, P. Habenberger, A. Wolf, G. Bjørkøy, C. Pridans, J. Eickhoff, B. Klebl, B. H. Hoff, E. Sundby, Synthesis and development of highly selective pyrrolo[2,3-d] pyrimidine CSF1R inhibitors targeting the autoinhibited form, J. Med. Chem. 66 (2023) 6959–6980, https://doi.org/10.1021/acs.jmedchem.3c00428.

[17] F. Lovering, Escape from Flatland 2: complexity and promiscuity, MedChemComm 4 (2013) 515–519, https://doi.org/10.1039/C2MD20347B.

[18] F. Lovering, J. Bikker, C. Humblet, Escape from flatland: increasing saturation as an approach to improving clinical success, J. Med. Chem. 52 (2009) 6752–6756, https://doi.org/10.1021/jm901241e.

[19] W.P. Walters, J. Green, J.R. Weiss, M.A. Murcko, What do medicinal chemists actually make? A 50-year retrospective, J. Med. Chem. 54 (2011) 6405–6416, https://doi.org/10.1021/jm200504p.

[20] B. Cox, V. Zdorichenko, P.B. Cox, K.I. Booker-Milburn, R. Paumier, L.D. Elliott, M. Robertson-Ralph, G. Bloomfield, Escaping from flatland: substituted bridged pyrrolidine fragments with inherent three-dimensional character, ACS Med. Chem. Lett. 11 (2020) 1185–1190, https://doi.org/10.1021/acsmedchemlett.0c00039.

[21] N. Frank, J. Nugent, B.R. Shire, H.D. Pickford, P. Rabe, A.J. Sterling, T. Zarganes-Tzitzikas, T. Grimes, A.L. Thompson, R.C. Smith, C.J. Schofield, P.E. Brennan, F. Duarte, E.A. Anderson, Synthesis of meta-substituted arene bioisosteres from [3.1.1]propellane, Nature 611 (2022) 721–726, https://doi.org/10.1038/s41586-022-05290-z.

[22] D. Dibchak, M. Snisarenko, A. Mishuk, O. Shablykin, L. Bortnichuk, O. Klymenko-Ulianov, Y. Kheylik, I.V. Sadkova, H.S. Rzepa, P.K. Mykhailiuk, General synthesis of 3-azabicyclo[3.1.1]heptanes and evaluation of their properties as saturated bioisosteres, Angew. Chem. Int. Ed. n/a (2023), e202304246, https://doi.org/10.1002/anie.202304246.

[23] D.F. Fernandez, M. Gonzalez-Esguevillas, S. Keess, F. Schafer, J. Mohr, A. Shavnya, T. Knauber, D.C. Blakemore, D.W.C. MacMillan, Redefining the synthetic logic of medicinal chemistry. Photoredox-catalyzed reactions as a general tool for aliphatic core functionalization, Org. Lett. (2023), https://doi.org/10.1021/acs.orglett.3c00994.

[24] M. Ishikawa, Y. Hashimoto, Improvement in aqueous solubility in small molecule drug discovery programs by disruption of molecular planarity and symmetry, J. Med. Chem. 54 (2011) 1539–1554. http://pubs.acs.org/doi/abs/10.1021/jm101356p.

[25] T.I. Aarhus, J. Eickhoff, B. Klebl, A. Unger, J. Boros, A. Choidas, M.-L. Zischinsky, C. Wolowczyk, G. Bjørkøy, E. Sundby, B.H. Hoff, A highly selective purine-based inhibitor of CSF1R potently inhibits osteoclast differentiation, Eur. J. Med. Chem. 255 (2023), 115344, https://doi.org/10.1016/j.ejmech.2023.115344.

[26] A.C. Reiersølmoen, J. Han, E. Sundby, B.H. Hoff, Identification of fused pyrimidines as interleukin 17 secretion inhibitors, Eur. J. Med. Chem. 155 (2018) 562–578, https://doi.org/10.1016/j.ejmech.2018.06.019.

[27] F. Bjørnstad, E. Sundby, B.H. Hoff, Directed lithiation of protected 4-chloropyrrolopyrimidine: addition to aldehydes and ketones aided by bis(2-dimethylaminoethyl)ether, Molecules 28 (2023) 932.

[28] B.A. Pollok, B.D. Hamman, S.M. Rodems, L.R. Makings, Optical Probes and Assays, 2000. WO 2000066766 A1.

[29] G.D. Diana, P. Rudewicz, D.C. Pevear, T.J. Nitz, S.C. Aldous, D.J. Aldous, D. T. Robinson, T. Draper, F.J. Dutko, Picornavirus inhibitors: trifluoromethyl substitution provides a global protective effect against hepatic metabolism, J. Med. Chem. 38 (1995) 1355–1371, https://doi.org/10.1021/jm00008a014.

[30] R.A. Hartz, V.T. Ahuja, X. Zhuo, R.J. Mattson, D.J. Denhart, J.A. Deskus, V. M. Vrudhula, S. Pan, J.L. Ditta, Y.-Z. Shu, J.E. Grace, K.A. Lentz, S. Lelas, Y.-W. Li, T.F. Molski, S. Krishnananthan, H. Wong, J. Qian-Cutrone, R. Schartman, R. Denton, N.J. Lodge, R. Zaczek, J.E. Macor, J.J. Bronson, A strategy to minimize reactive metabolite formation: discovery of (S)-4-(1-Cyclopropyl-2-methoxyethyl)-6-[6-(difluoromethoxy)-2,5-dimethylpyridin-3-ylamino]-5-oxo-4,5-dihydropyrazine-2-carbonitrile as a potent, orally bioavailable corticotropin-releasing factor-1 receptor antagonist, J. Med. Chem. 52 (2009) 7653–7668, https://doi.org/10.1021/jm900716v.

[31] M.P. Gleeson, Generation of a set of simple, interpretable ADMET rules of thumb, J. Med. Chem. 51 (2008) 817–834, https://doi.org/10.1021/jm701122q.

[32] M.W. Karaman, S. Herrgard, D.K. Treiber, P. Gallant, C.E. Atteridge, B.T. Campbell, K.W. Chan, P. Ciceri, M.I. Davis, P.T. Edeen, R. Faraoni, M. Floyd, J.P. Hunt, D. J. Lockhart, Z.V. Milanov, M.J. Morrison, G. Pallares, H.K. Patel, S. Pritchard, L. M. Wodicka, P.P. Zarrinkar, A quantitative analysis of kinase inhibitor selectivity, Nat. Biotechnol. 26 (2008) 127–132, https://doi.org/10.1038/nbt1358.

[33] M. Chartier, T. Chénard, J. Barker, R. Najmanovich, Kinome Render: a stand-alone and web-accessible tool to annotate the human protein kinome tree, PeerJ 1 (2013) e126, https://doi.org/10.7717/peerj.126.

[34] T.A. Halgren, R.B. Murphy, R.A. Friesner, H.S. Beard, L.L. Frye, W.T. Pollard, J. L. Banks, Glide: a new approach for rapid, accurate docking and scoring. 2. Enrichment factors in database screening, J. Med. Chem. 47 (2004) 1750–1759, https://doi.org/10.1021/jm030644s.